INFORMATION TO USERS

NOTE TO USERS

The original manuscript received by UMI contains broken, slanted and or light print. All efforts were made to acquire the highest quality manuscript from the author or school. Pages were microfilmed as received.

This reproduction is the best copy available

UMI

University of Alberta

Performance Analysis of Multivariable Processes

by

Amy Yiu ©

A thesis

submitted to the Faculty of Graduate Studies and Research

in partial fulfillment of the requirements for the degree of

Master of Science

in

Process Control

Department of Chemical and Materials Engineering

Edmonton, Alberta

Fall 1998

University of Alberta

Library Release Form

Name of Author: **Amy Yiu**

Title of Thesis: **Performance Analysis of Multivariable Processes**

Degree: **Master of Science**

Year This Degree Granted: **1998**

Permission is hereby granted to the **University of Alberta Library** to reproduce single copies of this thesis and to lend or sell such copies for private. scholarly or scientific research purpose only.

The author reserves all other publication and other rights in association with the copyright in the thesis. and except as hereinbefore provided neither the thesis nor any substantial portion thereof may be printed or otherwise reproduced in any material form whatever without the author's prior written permission.

....

Address:

#205. 15507-87 Avenue

Edmonton. Alberta

Canada T5R 4K5

Date: October 2. 1998
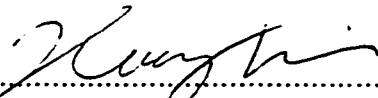
University of Alberta

Faculty of Graduate Studies and Research
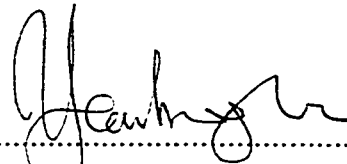
The undersigned certify that they have read. and recommend to the Faculty of Graduate Studies and Research for acceptance. a thesis entitled **Performance Analysis of Multivariable Processes** submitted by **Amy Yiu** in partial fulfillment of the requirements for the degree of **Master of Science** in Process Control.

....
Dr. S.L. Shah (Supervisor)

....
Dr. B. Huang

....
Dr. Y. Wu

(Dept. of Mathematical Sciences)

Date: October 2. 1998

Abstract

This thesis is concerned with the methods of process monitoring and control loop performance assessment. Statistical process control, as well as performance assessment method based on minimum variance benchmark are discussed. Various measures are developed to assist performing assessment for feedback and feedforward-feedback control systems. Effect of deviation of process delay estimate on the feedback performance measure is also investigated. In addition, a system identification based method for assessing the performance of multivariate closed-loop systems is proposed. The method uses *a priori* knowledge of the delays between different input-output pairs of the process and performs assessment on each individual loop separately. Results indicate that for cases with insignificant interaction between disturbances, this new technique could be used in place of existing multivariate techniques that require *a priori* knowledge of the unitary interactor matrix.

The practicality of the methods presented in this thesis are demonstrated using simulated, experimental and industrial data.

TO MY PARENTS

Mr. Yiu Kin Wah
Mrs. Wu Mui Lai

Contents

List of Figures

List of Tables

Chapter 1

Introduction

1.1 Overview of Control Loop Performance Assessment

Process and controller performance monitoring play important roles in determining the success of control applications. Control engineers spend a significant amount of time in the diagnosis of process variations, assessment of control application, and development of corrective strategies. In industries where there are a large number of control loops, having specialized tools for process monitoring and performance assessment would help control engineers perform their jobs more efficiently and effectively.

Recently, the area of control loop performance assessment has gained a lot of attention from researchers. Notable is the work of Harris (1989) who has shown that a lower bound on the closed-loop process variance, based on the concept of minimum variance control, could be obtained by analyzing routine closed-loop operating data. Desborough and Harris (1993) further extended the idea and defined a normalized performance index which indicates the performance of the overall feedback control scheme relative to the minimum variance benchmark. Huang (1997) developed an algorithm based on data filtering and correlation analysis to calculate a similar measure. Harris *et al.* (1996) applied the control performance analysis in an expert

system framework. The technique for feedback control loop has also been extended to feedforward-feedback systems by Desborough and Harris (1993) and Stanfelj *et al.* (1993).

Control loop performance assessment techniques have also been extended to multivariable processes. Huang *et al.* (1995) and Harris *et al.* (1996) proposed a methodology based on the estimation of the interactor matrix of the multiple-input multiple-output (MIMO) system. Evaluation of controller performance is achieved by comparing it to the performance of a MIMO minimum variance control system.

1.2 Objective of Study

The purpose of this thesis is:

1. to outline and discuss the use of traditional statistical process control methods for process monitoring;

2. to review univariate performance assessment method and develop the statistical properties of the feedback control performance measure;

3. to introduce a feedforward "payout" measure and a feedforward plus feedback control performance index for determining the potential benefit of implementing feedforward control on an existing feedback control system;

4. to investigate the effect of process delay estimate on the univariate performance measure; and

5. to propose an algorithm for assessing performance of multivariate systems without the knowledge of the unitary interactor matrix.

1.3 Organization of Thesis

This thesis consists of seven chapters including this introductory chapter. It is recommended that Chapter 3 to 7 be read in the same numerical order since there are

2

some cross dependencies between these chapters. The contents of these chapters are summarized as follows:

Chapter 2 Several popular statistical methods for process monitoring are summarized, from basic assumptions to fundamental statistical concepts. The use of quality control charts to monitor process quality is also discussed. Time series analysis in both time and frequency domains are outlined and illustrated by an industrial example.

Chapter 3 Huang's (1997) performance assessment strategy for single-input single-output (SISO) feedback systems, as well as the FCOR algorithm for calculating the performance measure, is given. The statistical properties of this performance measure is also given and applied to an industrial process.

Chapter 4 A "payout" measure to determine the benefit of implementing feedforward control is introduced in this chapter. The method for predicting performance of a feedback plus feedforward control system is also presented. These methods are evaluated by applications to simulation, experimental and industrial examples.

Chapter 5 In this chapter, the performance index curve is introduced to investigate the effect of the delay mismatch in the feedback control performance index. The 95% confidence level bound given in Chapter 3 is also applied to determine the accuracy of the estimated measure.

Chapter 6 A new approach to perform assessment of multivariate control systems, without the need of knowing the interactor matrix in advance, is proposed. Simulation examples are presented to illustrate the application of this proposed technique. Results are compared to those generated from Huang's (1997) MIMO algorithm.

Chapter 7 This chapter summarizes the conclusions presented in Chapters 2 to 6, and suggests future directions for follow-up in research.

Chapter 2

Statistical Analysis of Process Data

2.1 Introduction

Product quality has direct impact on the amount of profit a manufacturer can make. Too low a product quality causes loss of sales whereas too high a quality results in losses typically due to over-consumption of energy for production purposes. Therefore, it is essential to maintain product quality within a range of target values. Various statistical techniques have been devised over the years to achieve this purpose.

This chapter summarizes a few of the commonly used statistical methods for process monitoring. The basic assumptions made in developing these techniques are presented in Section 2.2. In Section 2.3, the fundamental statistical concepts are reviewed. Quality control charts and time series analysis are discussed in Sections 2.4 and 2.5 respectively. Time series analysis techniques are demonstrated on an industrial example in Section 2.6, followed by some concluding remarks in Section 2.7.

2.2 Basic Assumptions

Many statistical theories are based on two fundamental assumptions on the sampling method and the nature of the continuous signal being sampled. One assumption

is that samples are taken at a fixed frequency; that is, the time interval between each sample is constant. This assumption may not be exactly true but so long as the variations in sampling rate are small relative to the basic sampling interval, it is acceptable to assume constant sampling periods.

On a practical matter, one is often constrained to perform analysis based on limited amounts of data. Here, the implicit assumption is that the data used for analysis truly represent the long term nature of the signal being analyzed. This assumption can only be made if the process is strictly stationary, or at least weakly stationary (Pryor, 1982). This means that information acquired and analyzed today will give the same results as the information acquired in the future.

In the following sections, the expressions for estimating statistical functionals based on finite set of samples are introduced. The expressions for calculating the exact values of these functionals will not be considered. However, they can be easily found in most of the introductory statistics and time series analysis textbooks.

2.3 Fundamental Statistical Concepts

2.3.1 Mean and Error

Assume that a set of discrete data have been collected from a process. The simplest and easiest piece of information that can be determined from these data is the average value, which is also called the mean value. This is calculated by dividing the sum of all the values by the number of data points. Mathematically, this value is represented as

$$\bar{x} = \frac{1}{n} \sum_{t=1}^{n} x_t \tag{2.1}$$

where $\bar{x}$ is the average value, x_t is the value of t-th sample, and n is the number of samples. If the sampled variable is being regulated about a setpoint by a feedback controller, the average value of the data set would be expected to be equal to the setpoint. If the average is far from the control target, this indicates that the controller

5

does not perform well enough to have the process variable track the setpoint on average.

In any process, variability of the output is unavoidable. Another piece of information that can be obtained from process data is the variation about the average value of the data set. In order to determine how far a data point deviates from the average value, the error of that data point is calculated. The error is defined to be the difference between each data point and the average value of all the data points. The value of these errors can be both positive and negative. The total of the absolute value of the errors, that is, without regard to positive or negative deviations, divided by the number of samples will give the average value of the absolute error. Mathematically, this is

$$e_t = x_t - \bar{x} \tag{2.2}$$

$$\bar{e} = \frac{1}{n} \sum_{t=1}^{n} |e_t| = \frac{1}{n} \sum_{t=1}^{n} |x_t - \bar{x}| \tag{2.3}$$

where $\bar{e}$ is the mean absolute deviation, and e_t is the deviation of t-th measurement from the average. A large mean deviation indicates that there is a lot of variation about the average, while a small mean deviation reveals that the signal is fairly steady.

2.3.2 Variance and Standard Deviation

Two other most commonly used measures of data variation are the variance and the standard deviation. The variance of a sample of n measurements is defined to be

$$\sigma^2 = \frac{1}{n-1} \sum_{t=1}^{n} e_t^2 = \frac{1}{n-1} \sum_{t=1}^{n} (x_t - \bar{x})^2 \tag{2.4}$$

where σ^2 is the sample variance. Squaring the errors automatically converts them into positive numbers, and hence variance is always a finite positive number. The sample standard deviation σ is simply the square root of the variance:

$$\sigma = \sqrt{\frac{1}{n-1} \sum_{t=1}^{n} (x_t - \bar{x})^2} \tag{2.5}$$

The sample standard deviation is of great interest only when the distribution of values about the mean value of samples is assumed normal. That is, if a histogram of the number of samples occurring with any given value of e_t is plotted, a graph of a bell-shaped curve will be obtained. This curve is related to the standard deviation in the following manner:

- 68.3 percent of all values of e_t lie within one standard deviation from the mean $\bar{x}$

- 95.4 percent of all values of e_t lie within two standard deviations from the mean $\bar{x}$

- 99.7 percent of all values of e_t lie within three standard deviations from the mean $\bar{x}$

As far as improving quality control is concerned, it is naturally targeted towards reductions in standard deviation or the variance.

2.4 Quality Control Charts

Statistical process control charts such as the Shewhart and Cusum charts have been used extensively to monitor product quality and detect special events that may indicate out-of-control situations. Several of these techniques are highlighted below.

2.4.1 The Shewhart Chart

One important tool in statistical quality control is the Shewhart control chart. This control chart consists of a plot of time-series of the data as shown in Figure 2.1. Its most important merit is to ensure that data are displayed and not buried, with the indication of how much variation about the target value T can be expected to occur. This helps to avoid both over-reaction and under-reaction to apparent peculiarities in the data.

7
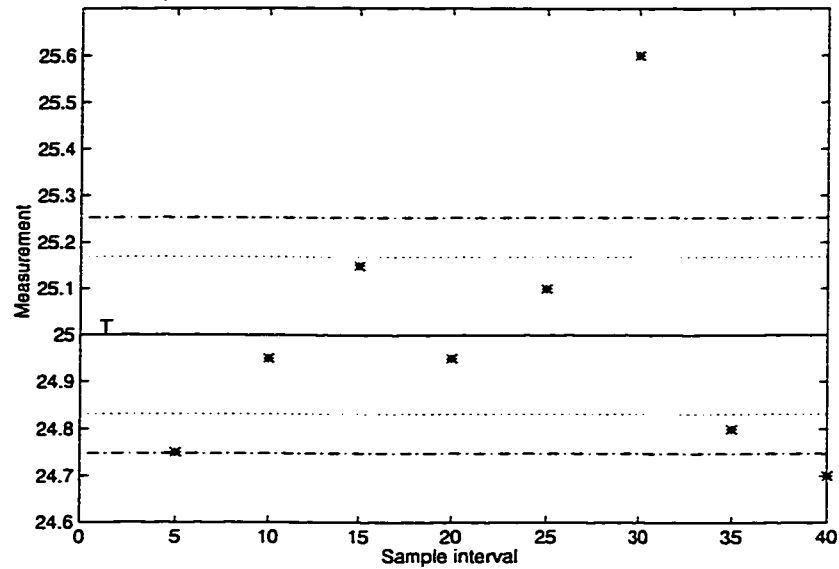
Figure 2.1: Example of a Shewhart control chart.

The control chart shown in Figure 2.1 has a solid line to indicate the target value. It also consists of a pair of dash-dotted lines called the action limits and a pair of dotted lines called the warning limits. If the measured quality characteristic is assumed to vary normally with one standard deviation σ, the action lines are usually centered on the target value T at $T \pm 3\sigma$. These are the 99.7 percent limit lines. The warning limits are usually the 95.4 percent lines at $T \pm 2\sigma$. The value of σ used in drawing these control lines is calculated when the process is *in control*, that is, when it is varying free of known disturbances (Box *at el.*, 1978).

Both the action and the warning limits are essential parts of a Shewhart control chart. Whenever a point lies outside the action limits, or two points in succession fall outside the warning limits, a cause of variation is likely to have occurred, and the performance target is not achieved. Investigation of the source and the mechanism of the variation may be needed.

Details of routine construction and use of quality control charts can be found in Grant and Leavenworth (1980).

8

2.4.2 The Cusum Chart

When changes of a specific kind are expected, additional charts that are more sensitive to this particular kind of change may be employed. For detecting small changes in mean level of an approximately normal process, the cumulative sum chart (Cusum) is more sensitive than the Shewhart chart.

A Cusum chart provides a means of presenting visually at any instant, the apparent mean of any group of consecutive points. In this chart, changes in the mean are detected by keeping a cumulative total of deviations from the target value T, that is, plotting the cumulative sum

$$S_n = \sum_{t=1}^{n} e_t = \sum_{t=1}^{n} (x_t - T) \qquad (2.6)$$

against n, the total number of samples recorded. Since the mean, relative to T, of the last r points is $(S_n - S_{n-r})/r$, it is obtained by joining the last point to the $(n-r)$th point and measuring the slope of the line. When a process is on target, e_t is a random error with zero mean. Suppose that at some intermediate time, $t = m$, the mean of the process shifted to a new value $T + \delta$. Then, at time m,

$$S_n = \sum_{t=1}^{n} e_t + (n-m)\delta \qquad (2.7)$$

for $m < n$. Besides the random sum, there is now a systematic component $(n-m)\delta$ increasing steadily with each new data point. Thus a change in mean value of the process variable will be detected by a change in slope of the Cusum plot. In practice, locating the change is remarkably useful in helping to discover its cause. The bottom chart in Figure 2.2 shows the change in slope of the Cusum chart associated with the change in its mean value.

In order to determine when corrective action should be initiated, some kind of decision criterion is needed for the Cusum chart. The V-mask scheme, suggested by Barnard (1959), provides a simple two-sided test for quality specifications. A V-shaped mask is superimposed on the Cusum chart with the vertex pointing forwards, and set at a distance d ahead of the most recent point, as shown in Figure 2.3. The

9
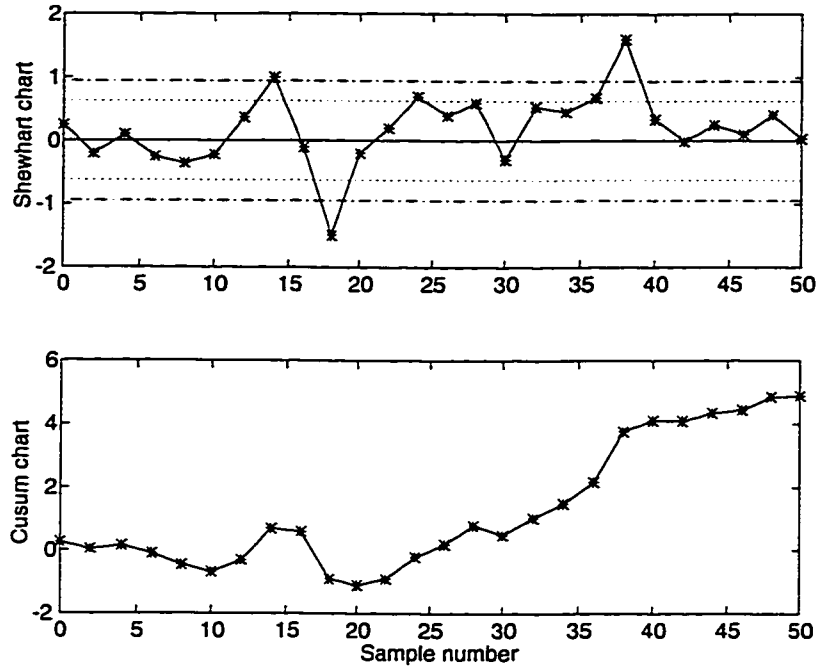
Figure 2.2: Comparison of Shewhart and Cusum charts.

angle between the obliques and the horizontal is denoted by θ. If all the previous plotted points fall within the V, the process is assumed to be in control. If some of the points cross one of the limbs of the V, a search for causes of variation is initiated. The construction of V-mask is described in Ewan (1963) and Wetherill (1969).

2.4.3 The Mosum Chart

Despite the Cusum chart being an effective and common tool for process monitoring, it tends to "desensitize" as time progresses due to its very definition. All past observations contribute to the test statistics, so that the relative weight of the observations after a violation of constancy decreases with increasing time of the onset of the violation. Further, the form of the significance limits for the simultaneous test of the Cusums are nonlinear over time (Bauer and Hackl, 1978).

These problems, however, can be overcome by using moving sums (Mosums) of recursive residuals, with the sum of a fixed number of past residuals being taken as

10
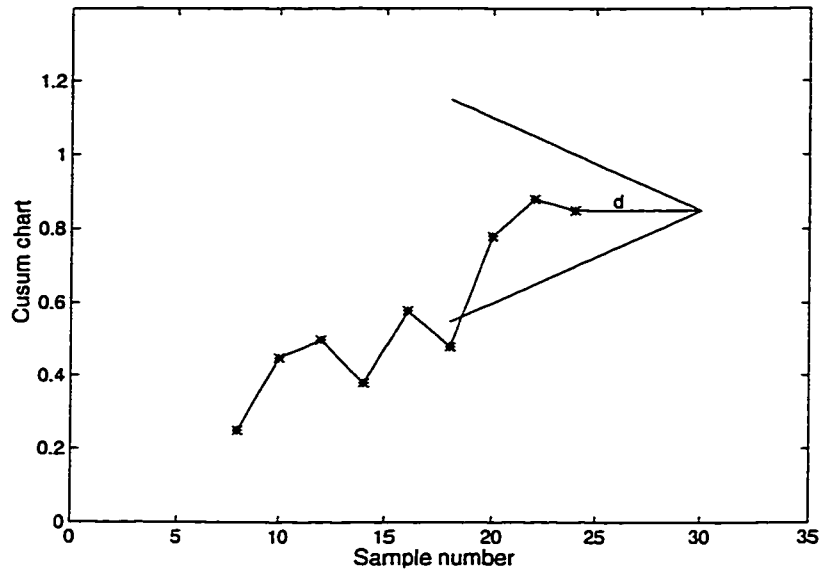
Figure 2.3: The use of a V-mask on a Cusum chart.

a test criterion at each point of time. Since a window of observations of fixed width is tested at each point in time, the significance limits for the simultaneous test of the Mosums can be assumed constant over time if the dependency between the Mosums is ignored, and if the variance of the process is known (Bauer and Hackl, 1978).

There are other quality control methods, such as exponentially weighted moving average (EWMA) and exponentially weighted moving variance (EWMV), that provide useful tools for process monitoring. These schemes, in some situations, are proved to outperform the Shewhart and the Cusum charts (Crowder and Hamilton, 1992, MacGregor and Harris, 1993).

2.5 Time Series Analysis

Consider two sinusoids, each with the same amplitude but different frequencies. In other words, they have the same statistical mean, variance and standard deviation. They, however, represent very different types of processes, and thus represent very different control problems.

11

One needs to know whether the variability of a process is fast or slow, and how fast or how slow. Before starting, the frequency of variations to be analyzed has to be estimated so that the sampling period, together with the total time for sampling, can be determined. The following two rules should be followed when sampling (Pryor, 1982):

1. Samples must be taken at least twice as often as the highest frequency to be analyzed. For example, if disturbances up to one cycle per second are to be analyzed, one must sample at least two times per second.

2. Samples must be taken for at least eight cycles of the lowest frequency to be analyzed. That is, if disturbances down to one cycle per minute are to be analyzed, samples must be taken for at least eight minutes.

Once the data have been collected, time series analysis can be carried out.

Time series analysis refers to techniques dealing with the analysis of data from random observations with time or space as characteristic. It can be done either in the time domain or in the frequency domain. Some of the most important functions generated in a time series analysis are discussed in this section.

2.5.1 Autocovariance and Autocorrelation

Autocovariance is an indication of how fast a signal is varying. For a finite data record, the equation for evaluating autocovariance is

$$\gamma_{xx}(j) = \frac{1}{n} \sum_{t=1}^{n-j} (e_t e_{t+j}) \tag{2.8}$$

where $\gamma_{xx}(j)$ denotes the autocovariance at j lags, and j varies from 0 to $n - 1$. If j is equal to zero, then

$$\gamma_{xx}(0) = \frac{1}{n} \sum_{t=1}^{n} (e_t e_t) = \sigma^2 \tag{2.9}$$

which is simply the process variance.

12

Since e_t can be positive when e_{t-j} is negative, there can be negative values in the summation of Equation 2.8. Therefore, the more often the error changes sign, the more likely the negative terms will occur in the summation equation, and the smaller will the resulting autocovariance be. For this reason, all autocovariance values are always smaller than the variance. In fact, autocovariance can be negative.

The results of autocovariance analysis can be presented graphically by plotting the autocovariance functions against the lags as shown in the bottom graph of Figure 2.4. The time series plot is presented in the top graph for comparison. Inasmuch as autocovariance is symmetric about the ordinate, the plot is usually shown for positive lags only. The positions of the peaks and valleys depend on the frequency of the variations in the error. Therefore, major frequencies of the process disturbances can simply be determined by inspecting the plot visually. For instance, if the sample interval is one second, and a peak occurs at 5 lags, then there is a disturbance occurring at a rate of once every 5 seconds, or 0.2 Hz.

The autocovariance function is dependent on the unit of measurement and this makes the comparison of different time series difficult. The autocorrelation function, which is unitless, is therefore more widely used than the autocovariance function. It is easily calculated by normalizing the autocovariance by the variance, that is,

$$\rho_{xx}(j) = \frac{\gamma_{xx}(j)}{\gamma_{xx}(0)} \tag{2.10}$$

where $\rho_{xx}(j)$ is the autocorrelation at j lags.

The autocorrelation function quantifies the similarity between neighboring values. A value of $\rho_{xx}(j)$ close to $+1$ implies strong similarity or dependence in the same direction between pairs of values of a variable separated by lag j. A value close to zero indicates no similarity; whereas a value close to -1 indicates strong similarity but in the opposite direction. The autocorrelation function is usually plotted against lag j to generate an autocorrelogram.

Another use of the autocorrelation function is to show the effect of process control applications. A control system is expected to reduce the magnitude and alter the

13
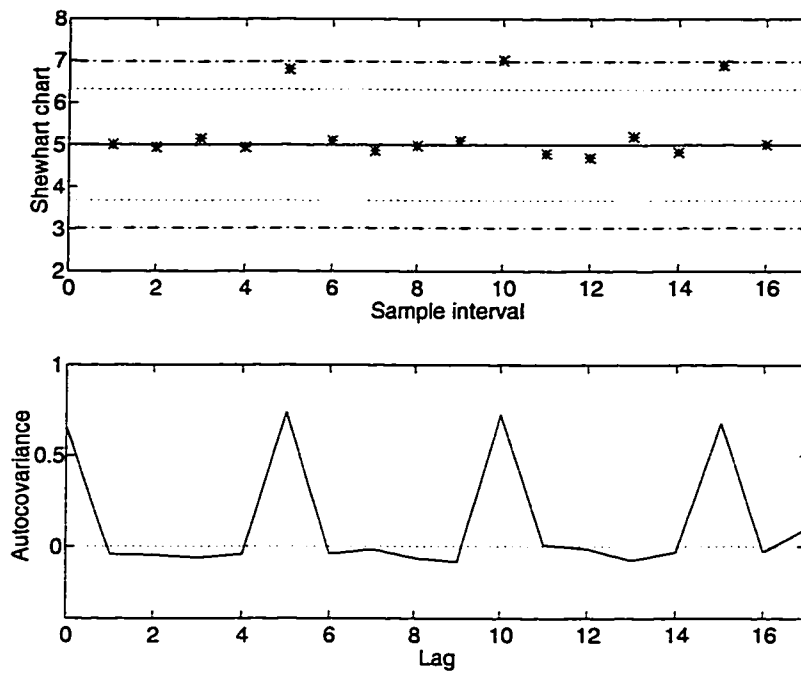
Figure 2.4: Relationship between the frequency of a disturbance and the locations of peaks in an autocovariance plot.

nature of the process variations. Thus its effect should be reflected in a corresponding change in the autocorrelogram of the process.

2.5.2 Power Spectrum

The introduction of the spectral density accomplishes a mapping of the properties of a stochastic process from the time domain to corresponding properties in the frequency domain. By taking the Fourier transform of the autocovariance function, one can derive the power spectral density or simply the power spectrum which expresses the energy content of a process signal as a function of frequency. Since the main interest lies in the application of the power spectrum, the mathematics of the transformation will not be discussed.

Peaks in the power spectrum curve show the frequencies at which there is a high contribution to the variation. Thus, a single narrow peak suggests a possible periodicity in the signal being studied. If there are harmonics, there will be a set of narrow peaks at frequencies which have a common denominator. With random variations, the spectrum will be flat across the frequencies.

One interesting characteristic of the power spectrum is that the area under the curve gives the variance $\gamma_{xx}(0)$. The percentage of the total area which lies between two frequencies is the same as the percentage of the variance that has been assigned to that frequency band. Therefore, the overall frequency range can be broken down into arbitrary bands to characterize the variation. By breaking down variations into components at different frequencies, the power spectrum can help identify their sources. In some cases the power spectrum may show cyclic components with periods, which might be related to readily identifiable events in the operation or to dominant frequencies identified in the power spectrum of another variable.

Comparison of power spectra can help identify relationships between variables. If considerable variations occur in both variables at common frequencies, it is most likely that either, one is causing the other or, they have a common cause. In case of the latter, further investigation can be narrowed down to factors or inputs known to

15

affect both variables.

2.5.3 Cross Correlation

The cross correlation function is a useful measure of similarity between two variables taken at different time lags. Given two stochastic processes x_t and y_t, which are jointly stationary, their similarity should only be a function of lag and is independent of time. In such cases, the cross covariance function between x_t and y_t is

$$\gamma_{xy}(j) = \frac{1}{n} \sum_{t=1}^{n-j} (x_t - \bar{x})(y_{t+j} - \bar{y}) \qquad (2.11)$$

in which $\bar{x}$ and $\bar{y}$ are the means of the x_t and y_t series, respectively.

The corresponding cross correlation is defined as

$$\rho_{xy}(j) = \frac{\gamma_{xy}(j)}{\gamma_{xx}(0)\gamma_{yy}(0)} \qquad (2.12)$$

It has similar usage to that of the autocorrelation except that pairs of values of two different variables are analyzed. The cross correlation also takes values between -1 and +1. The greater the similarity at a particular lag, the higher the absolute value of the cross correlation at that lag. The sign shows whether one increases or decreases with an increase in the other. A cross correlogram is often used to plot the cross correlation function against lag.

2.5.4 Coherence

Similar to the relationship between the power spectrum and the autocovariance, the cross spectrum is the Fourier transform of the cross covariance. The amplitude of the cross spectrum is known as the cross amplitude spectrum. The coherence or the squared coherency is defined as the ratio of the squared cross amplitude spectrum to the input spectrums. For a linear system, it can also be interpreted as the fraction of the output variation which is related to, or contributed by, the input variation at the given frequency. Coherence gives no indication of any phase difference between two variables.

Some salient properties and interpretations of coherence are (Nobleza, 1990):

1. It does not depend on the scales of measurement;

2. It does not show causality;

3. In an ideal case of a constant parameter linear system, that is, with a single clearly defined input and output, coherence at all frequency is unity;

4. The coherence function is zero for all frequencies if two processes are completely unrelated.

2.5.5 Coherent Power

The power spectrum reveals the variance component of a process variable at each frequency. On the other hand, the coherence function gives the fractional portion of the variance component of a process variable related to the other at each frequency. The coherent power (or sometimes coherent output power) which is the product of the power spectrum and the coherence function, would therefore give the portion of the variation in a process variable which is related to the other, at every frequency.

Coherent power highlights information of high coherence at frequencies which contain substantial variation at the same time. It eliminates information of high coherence at frequencies which do not have corresponding variation and also on variations which are not correlated. This function is useful because it is not only the degree of correlation between two variables that is of interest, but also the incidence of substantial variation that is highly correlated to the other variable. Inasmuch as the area under the power spectrum curve gives the variance, the area under the coherent power curve gives the part of the variance related to the other variable.

Some common functions in time series analysis, together with the information they provide, are summarized in Table 2.1.

Table 2.1: Functions generated by time series analysis (adapted from Nobleza *et al.*).

Autocorrelation (time domain)	- nature of variability: long term, short term - cyclic variations - control loop performance
Power spectrum (frequency domain)	- distribution of variance over the frequency range - nature of the variability: long term, short term - potential improvement from process control - control loop performance
Cross correlation (time domain)	- degree of relationship between variables - time lag between two processes - direction (sign) of the relationship
Coherence (frequency domain)	- degree of relationship between variables
Coherent power (frequency domain)	- proportion of the variance in a variable related to the variability of the other

2.6 Industrial Application

The above time series analysis techniques are demonstrated using data obtained from an industrial NO_2 production process. In this process, the synthesis of nitrogen dioxide from ammonia and air is carried out in a catalytic reactor. Ammonia is preheated by process steam in a superheater before being fed to the reactor. The variables being investigated are the catalyst temperature of the reactor (T106) and its major disturbances including the ammonia feed temperature (T212X) and flow rate (F128) and the pressure of the steam fed to the superheater (P007). The closed loop data of the process, sampled at ten second intervals over one day, are shown in Figure 2.5.

It can be observed from the time plot that there is a big perturbation to the catalyst temperature between 6000 and 7000 sample intervals. In order to identify the source of this disturbance, time series analysis as discussed in the previous section is performed. Figure 2.6 is the autocorrelogram of the catalyst temperature estimated between 6000 and 7000 sample intervals. The curve decays from its maximum of unity at lag zero to zero as the lag increases. The ripples indicate that the process has a periodic component with a period of approximately 850 seconds, or equivalently, 0.0012 Hz, .

Characteristics and periodicity of the variation revealed by its autocorrelation can be compared to that of the suspected source. In this NO_2 production process, the three major disturbances, T212X, F128 and P007, are examined for any correlation with the periodic component at T106. Their corresponding autocorrelograms as estimated for observations 6000 to 7000 are presented in Figures 2.7, 2.8 and 2.9 respectively.

From figure 2.8, it is apparent that there is no similar characteristics between the catalyst temperature and the ammonia flow. It only indicates that the ammonia flow consists of many high frequency variations which could be caused by the action of the flow controller. On the other hand, the peaks located at lag 85 in Figures 2.7

19
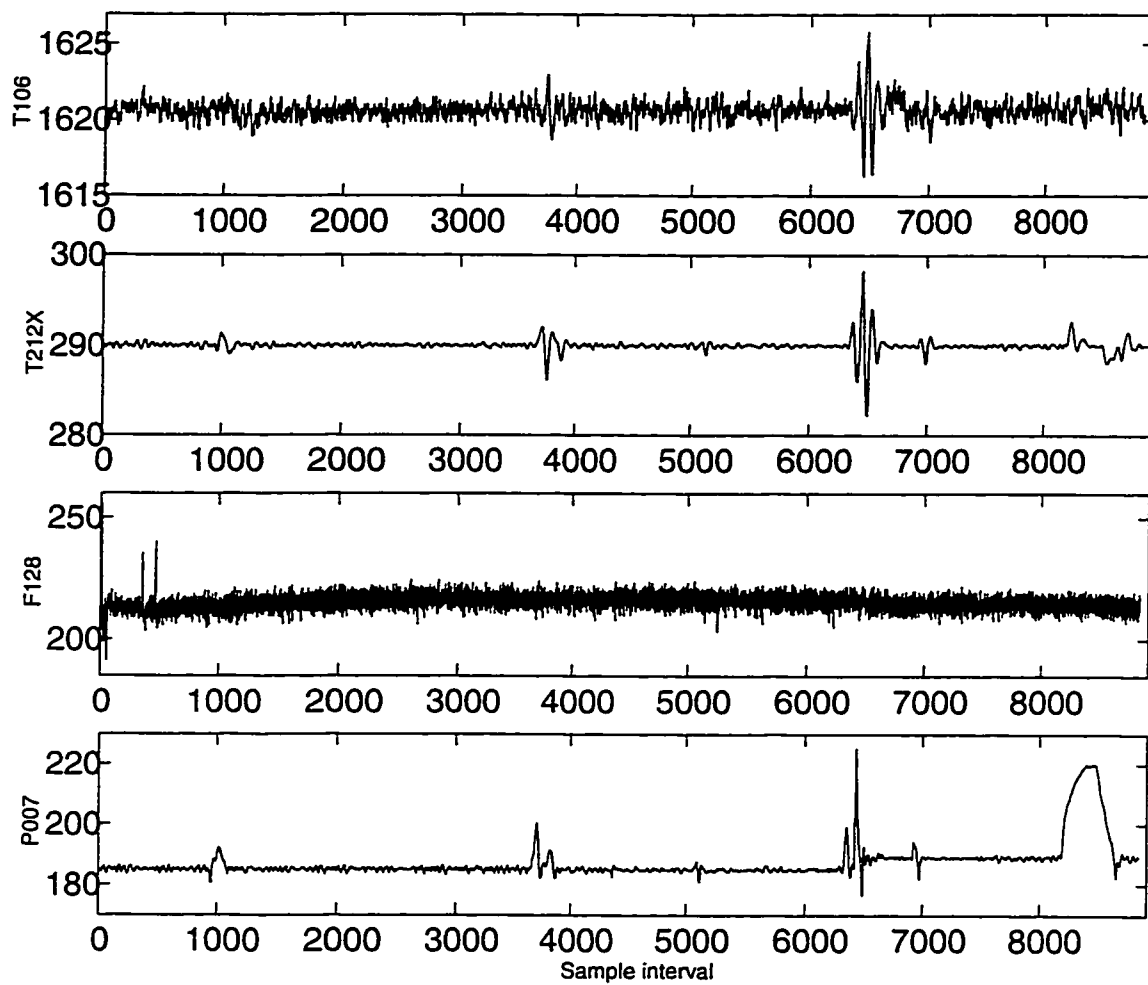
Figure 2.5: Time plots of the catalyst temperature, ammonia temperature, flow rate and steam pressure.
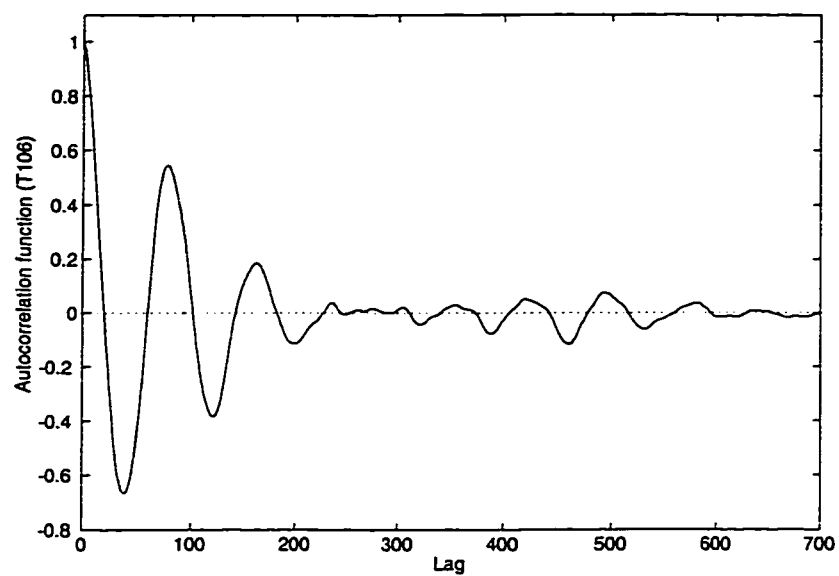
Figure 2.6: Autocorrelogram of the catalyst temperature.
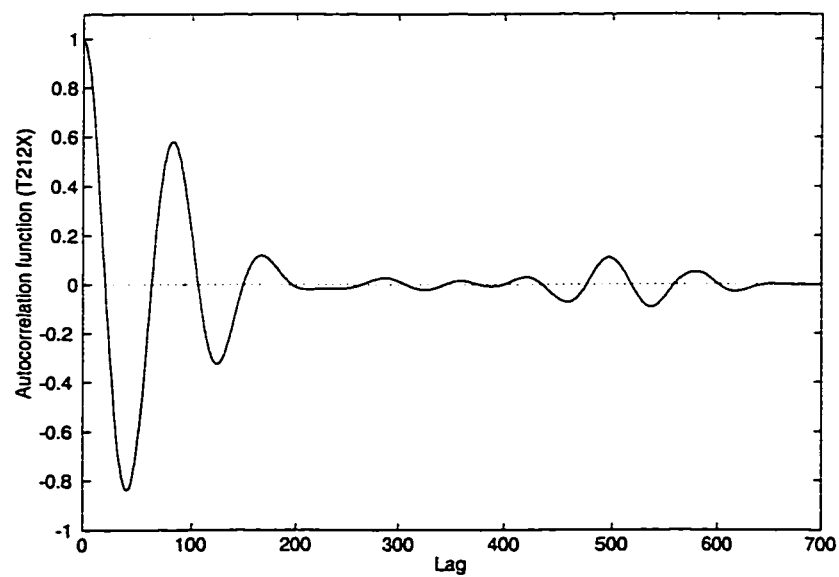
Figure 2.7: Autocorrelogram of the ammonia temperature.

21
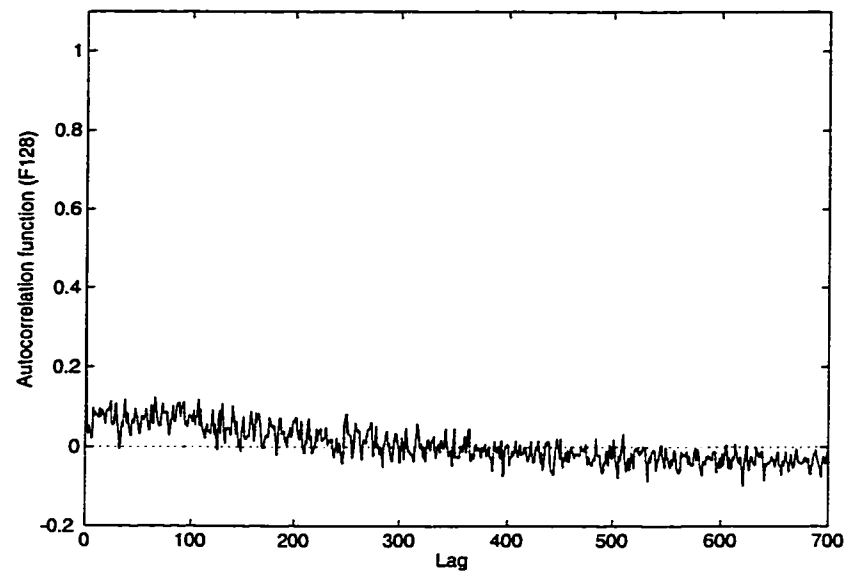
Figure 2.8: Autocorrelogram of the ammonia flow.
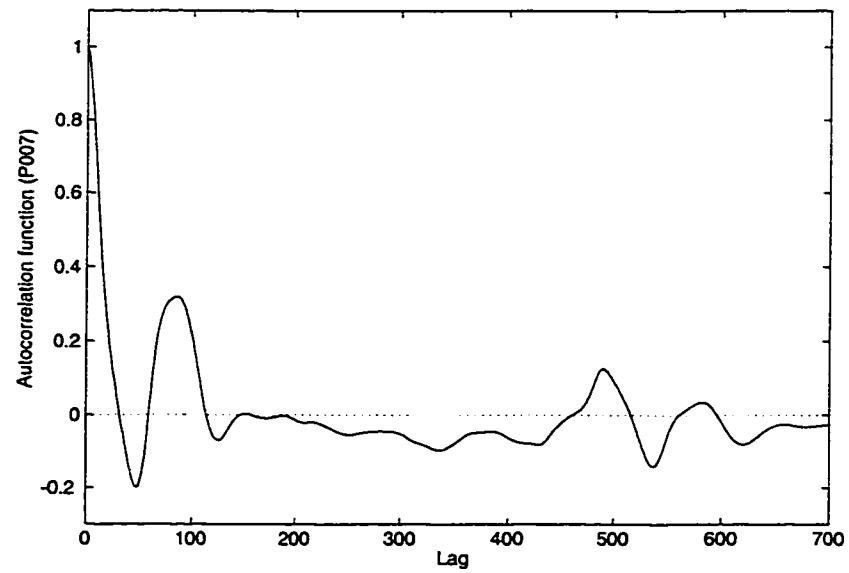
Figure 2.9: Autocorrelogram of the steam pressure.

and 2.9 indicate that both the ammonia feed temperature and the steam pressure possess a periodic component of 0.0012 Hz. The same phenomenon can also be seen from the power spectrum plots of the process variables, as given in Figures 2.10, 2.11, 2.12 and 2.13. The power spectrum plots of the catalyst temperature, the ammonia temperature and the steam pressure all reveal a narrow peak at 0.0012 Hz. This peak indicates the presence of a periodic variation of 0.0012 Hz. Therefore, it is highly probable that the ammonia temperature and the steam temperature, or either one of them is the cause of the disturbance to the catalyst temperature between 6000 and 7000 sample intervals. With random variation, the spectrum of the ammonia flow rate in Figure 2.12 is rather flat with power distributed across the frequencies.

Bivariate analysis is carried out to determine which of the two disturbances is the cause of the variation. It is suspected that the root source of this periodic variation is the steam pressure, which perturbs the ammonia temperature during the preheating process, which in turn affects the catalyst temperature of the reactor. The cross correlograms shown in Figures 2.14 and 2.15 prove that the catalyst temperature has a stronger correlation with the ammonia temperature than that of the steam pressure at lag 85. In addition, the coherence plot in Figure 2.16 reveals that more than 90 percent of the variation in the catalyst temperature having 0.0012 Hz frequency is contributed by the ammonia temperature under the assumption of linearity of the system.

The coherent power plot in Figure 2.17 shows the amount of variation in catalyst temperature related to the ammonia temperature. Comparison of the power spectrum of the catalyst temperature and its coherent power with the ammonia temperature indicates that a good portion of the low frequency components in the catalyst temperature are coherent to the ammonia temperature.

From the above univariate and bivariate statistical analyses, it can be concluded that the direct cause of the variations in the catalyst temperature between 6000 and 7000 sample intervals is the ammonia temperature. The root cause would most likely be the steam pressure since the steam is used to preheat the ammonia before the
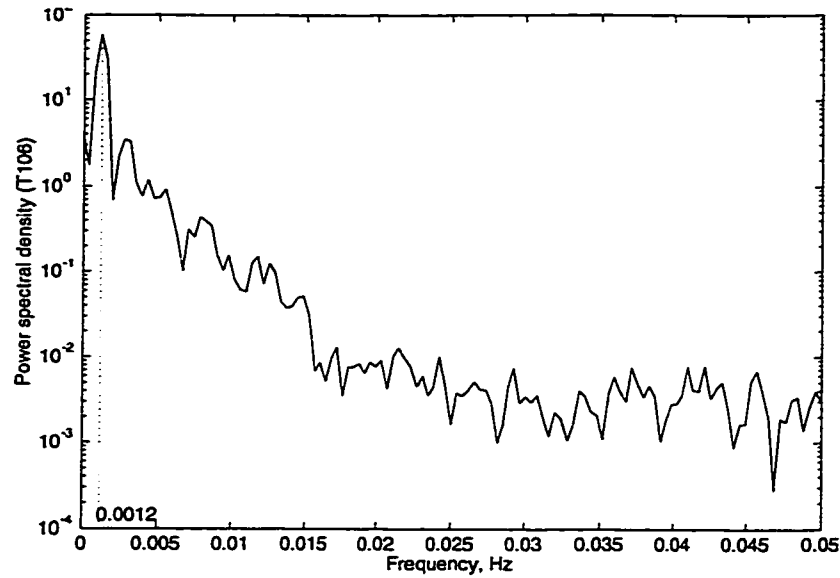
Figure 2.10: Power spectrum of the catalyst termperature.

ammonia is fed to the reactor.

2.7 Conclusions

It is frequently important to detect, identify and estimate major sources of variations when monitoring a process. In this chapter, time and frequency domains statistical analysis techniques directed towards these goals are studied. Control charts are especially helpful in detecting process variations. Time series analysis has proved itself useful in studying and identifying sources of disturbances in an industrial NO_2 production process. Both time domain and frequency domain analyses identified the ammonia temperature as the direct cause of the variations in the catalyst temperature.
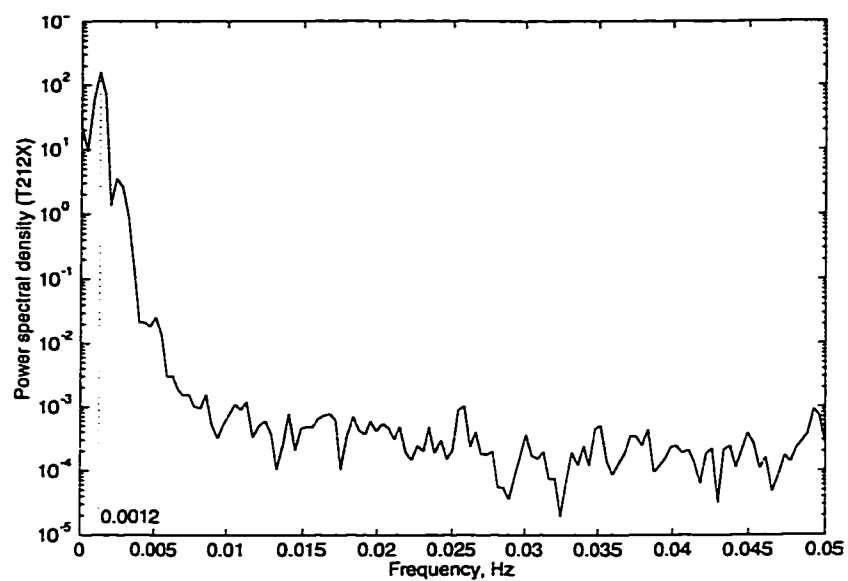
Figure 2.11: Power spectrum of the ammonia temperature.
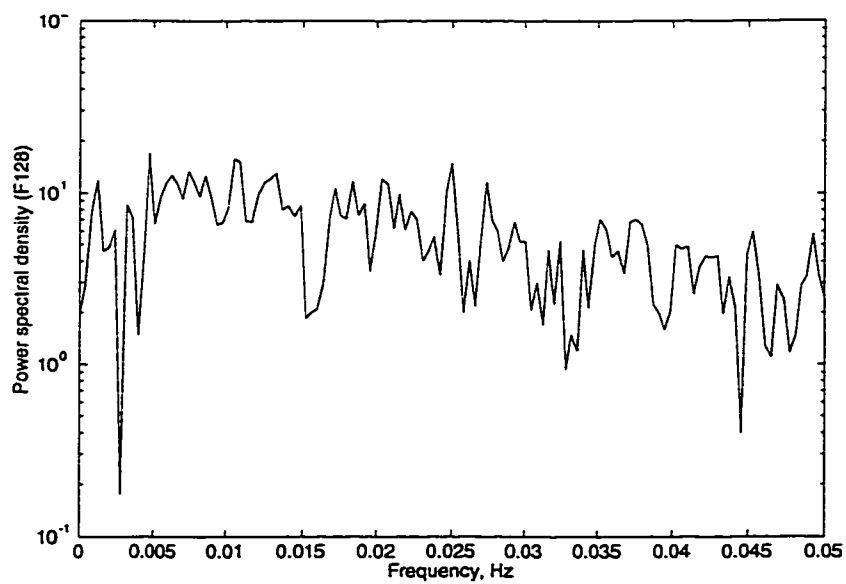
Figure 2.12: Power spectrum of the ammonia flow.
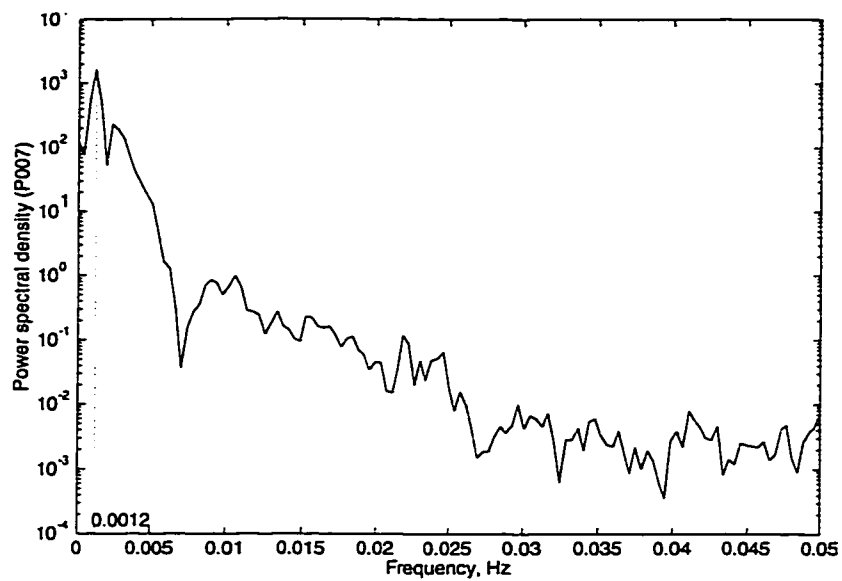
Figure 2.13: Power spectrum of the steam pressure.
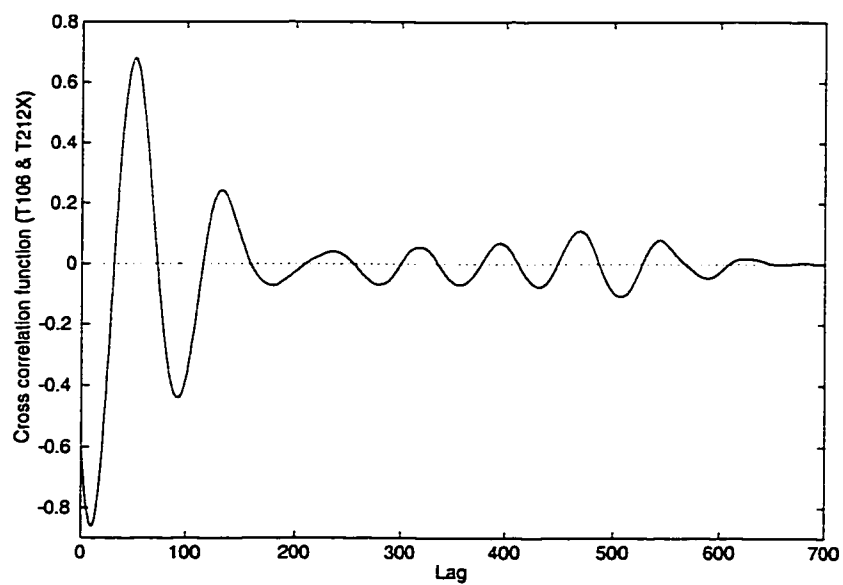
Figure 2.14: Cross correlogram showing relationship between the catalyst temperature and the ammonia temperature.
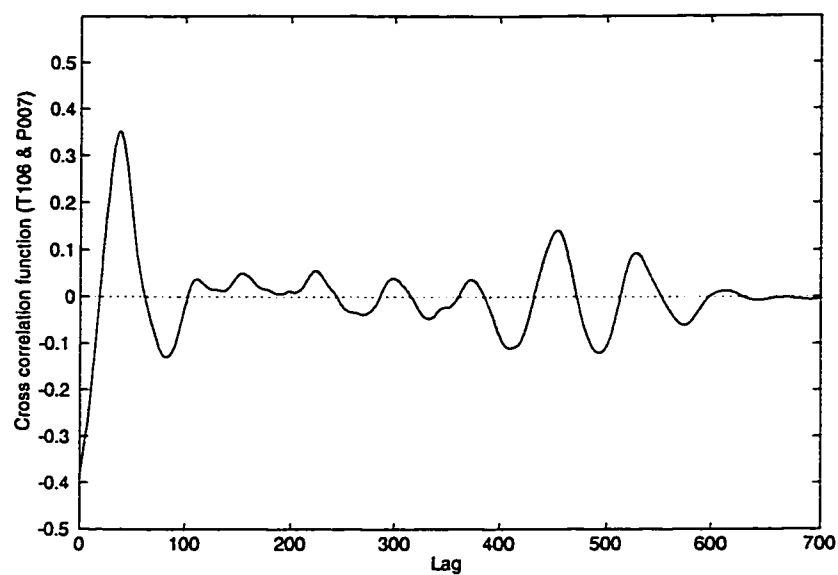
Figure 2.15: Cross correlogram showing relationship between the catalyst temperature and the steam pressure.
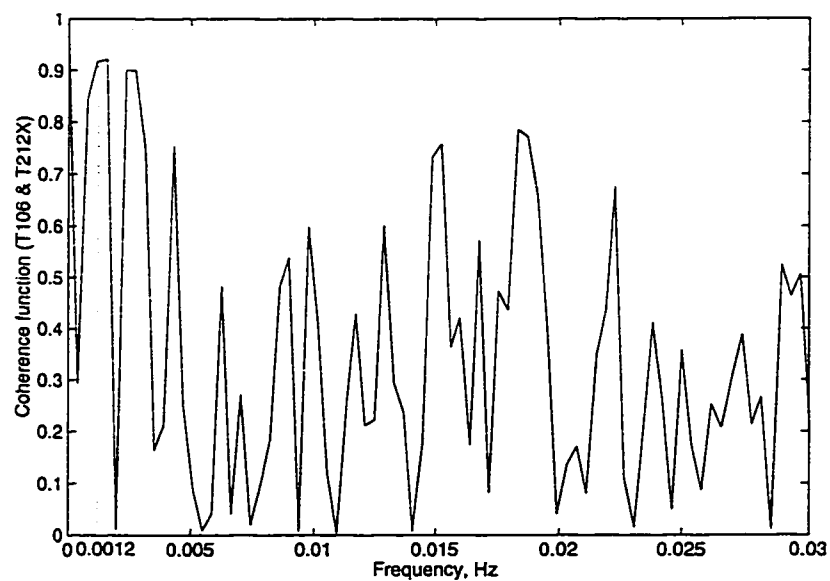
Figure 2.16: Coherence of the catalyst temperature with the ammonia temperature.

27
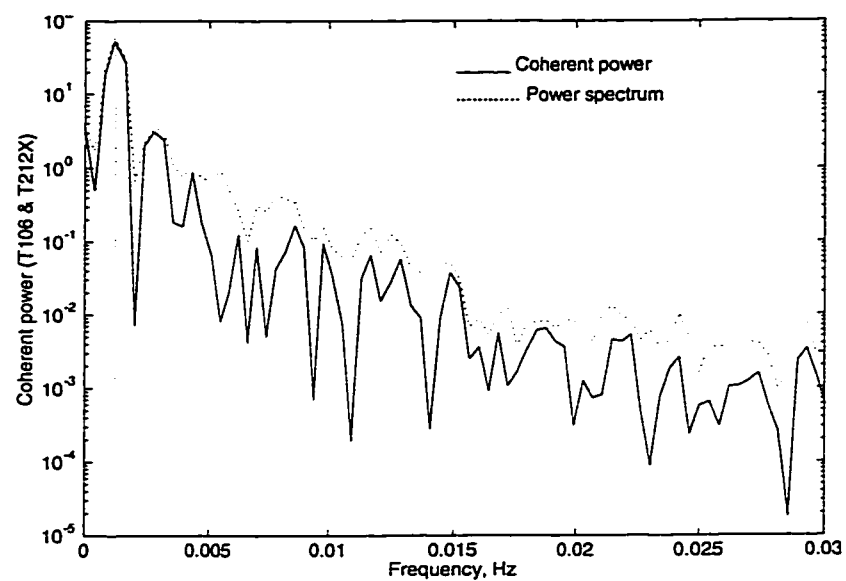
Figure 2.17: Coherent power of the catalyst temperature with the ammonia temperature.

Chapter 3

Performance Assessment of Univariate Feedback Control Loop

3.1 Introduction

In industries where there are a great number of control loops operating automatically, it would be convenient to have some formalized assessment tools to diagnose the performance of the control loops. The process variability analysis summarized in the previous chapter provides a means for monitoring control loop performance. There are also other techniques that make use of performance benchmarks to determine whether control systems are performing satisfactorily. These benchmarks can be user-specified, observed from historical data, or deduced from optimal control theories. The choice of a benchmark depends on the goals and requirements of the control application. For instance, if the speed of the output response reaching the setpoint is the main concern, one may wish to consider desired closed-loop dynamics such as settling time or overshoot as a reference benchmark.

Among all the performance benchmarks available, the most popular one is the minimum variance control. Its control objective is to minimize the variance of the process output. Minimum variance control is impractical in reality because of its excessive control action but it is extremely useful in providing a theoretical lower bound

on the output variance under linear feedback control. The performance measure using minimum variance control as benchmark was first established by Harris (1989) and was later modified by Huang in his Ph.D. thesis (1997). In Section 3.2 of this chapter, the formulation of the performance measure defined by Huang (1997) for single-input single-output case (SISO), as well as the FCOR algorithm for calculating this measure, is introduced. The statistical properties of this performance measure is discussed in Section 3.3. Finally, the technique is applied to an industrial process in Section 3.4.

3.2 Feedback Controller Performance Measure

The idea of minimum variance control can be easily explained and understood by considering a stable closed-loop system such as the one presented in Figure 3.1. Note that d is the process delay, $\widetilde{T}$ is the delay-free process transfer function, Q is the controller, N_a is the disturbance model and a_t is a white noise sequence with zero mean. The output response of the system is

$$y_t = \frac{N_a}{1 + q^{-d}Q\widetilde{T}}a_t \tag{3.1}$$

Long division yields an infinite order impulse response, or

$$y_t = (f_0 + f_1 q^{-1} + \cdots + f_{d-1}q^{-d+1} + f_d q^{-d} + \cdots)a_t \tag{3.2}$$

where f_0, f_1, ..., f_{d-1}, f_d, ... are the constant impulse response coefficients of y_t observed from a_t. The first d terms of the right hand side of Equation 3.2 are independent of the controller Q, and therefore are known as feedback controller invariant. These terms cannot be reduced or eliminated no matter what kind of controller is used. Thus they remain unchanged as long as there is no alteration in the physical configuration of the process, and the process delay is constant. The best a controller can ever do is to eliminate all the remaining terms after f_{d-1}. When this is the case, the system is described to be under minimum variance control.
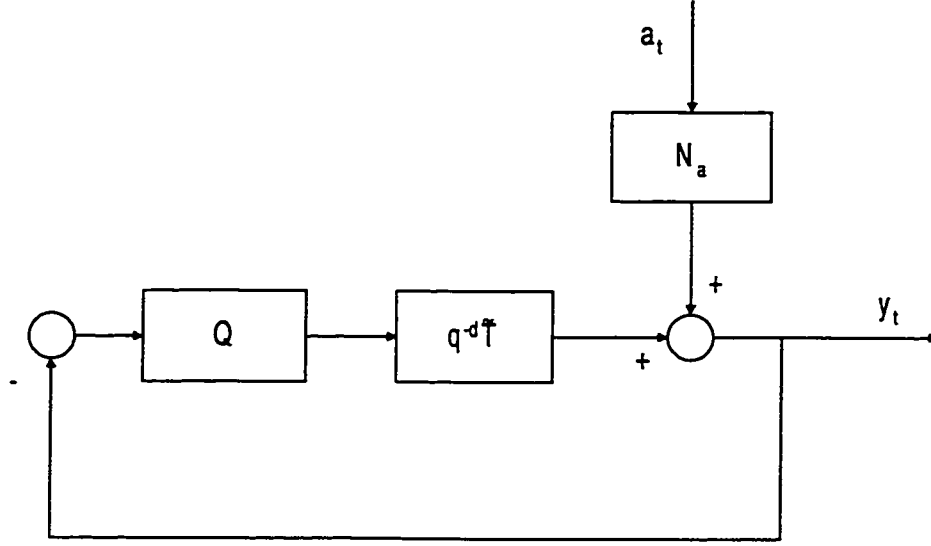
Figure 3.1: Block diagram of a closed-loop system.

Multiplying Equation 3.2 by a_t, a_{t-1}, ..., a_{t-d+1} respectively and then taking expectation on both sides results in the following equations:

$$\gamma_{ya}(0) = E[y_t a_t] = f_0 \sigma_a^2$$

$$\gamma_{ya}(1) = E[y_t a_{t-1}] = f_1 \sigma_a^2$$

$$\vdots$$

$$\gamma_{ya}(d-1) = E[y_t a_{t-d+1}] = f_{d-1} \sigma_a^2 \tag{3.3}$$

where $\gamma_{ya}(k)$, $k = 0, 1, ..., d-1$ is the cross covariance between y_t and a_t. Applying the above results in evaluating the minimum variance of the output gives

$$
\begin{aligned}
\sigma_{mv}^2 &= (f_0^2 + f_1^2 + \cdots + f_{d-1}^2)\sigma_a^2 \\
&= [(\frac{\gamma_{ya}(0)}{\sigma_a^2})^2 + (\frac{\gamma_{ya}(1)}{\sigma_a^2})^2 + \cdots + (\frac{\gamma_{ya}(d-1)}{\sigma_a^2})^2]\sigma_a^2 \\
&= \frac{\gamma_{ya}^2(0) + \gamma_{ya}^2(1) + \cdots + \gamma_{ya}^2(d-1)}{\sigma_a^2}
\end{aligned}
\tag{3.4}
$$

Using minimum variance as benchmark, the controller performance index is defined as

$$\eta(d) \triangleq \frac{\sigma_{mv}^2}{\sigma_y^2} \tag{3.5}$$

31

which is a function of process delay. Since the output variance σ_y^2 can never be smaller than the minimum variance σ_{mv}^2, $\eta(d)$ must be less than one. Indeed $0 \leq \eta(d) \leq 1$ is always valid. Whenever $\eta(d)$ is close to zero, it indicates that the performance of the current control loop is poor, and there is a great potential to reduce the process variance by retuning the controller. If $\eta(d)$ is close to one, the process is almost operating under minimum variance control, or at its optimal performance bound. Further improvement of the performance cannot be obtained by simply retuning the controller. Other control schemes or reconfiguration of the process should be considered.

Let $\rho_{ya}(0)$, $\rho_{ya}(1)$, ..., $\rho_{ya}(d-1)$ be the cross correlation coefficients between y_t and a_t for lags 0 to $d-1$, or

$$\rho_{ya}(k) = \frac{\gamma_{ya}(k)}{\sigma_y \sigma_a}, k = 0, 1, \ldots, d-1$$

Substituting Equation 3.4 into Equation 3.5 would yield

$$
\begin{aligned}
\eta(d) &= \frac{\gamma_{ya}^2(0) + \gamma_{ya}^2(1) + \cdots + \gamma_{ya}^2(d-1)}{\sigma_y^2 \sigma_a^2} \\
&= \rho_{ya}^2(0) + \rho_{ya}^2(1) + \cdots + \rho_{ya}^2(d-1) \\
&\triangleq X^T X
\end{aligned}
$$

(3.6)

where X is defined as

$$X \triangleq \begin{bmatrix} \rho_{ya}(0) \\ \rho_{ya}(1) \\ \vdots \\ \rho_{ya}(d-1) \end{bmatrix}$$

(3.7)

The sampled version of the performance index is

$$\widehat{\eta}(d) = \widehat{\rho}_{ya}^2(0) + \widehat{\rho}_{ya}^2(1) + \cdots + \widehat{\rho}_{ya}^2(d-1) = \widehat{X}^T \widehat{X}$$

(3.8)

where

$$\widehat{\rho}_{ya}(k) = \frac{\frac{1}{N} \sum_{t=k+1}^{N} y_t a_{t-k}}{\sqrt{\frac{1}{N} \sum_{t=1}^{N} y_t^2 \frac{1}{N} \sum_{t=1}^{N} a_t^2}}$$

(3.9)

is the sample correlation and N is the sample size.

Since a_t is unmeasurable, it must be estimated via time series analysis of the process output variable y_t. This procedure is known as Filtering and CORrelation analysis (FCOR) by Huang (1997). The estimated innovations sequence $\hat{a}_t$ can be evaluated by pre-whitening y_t by an AR or ARMA time series model or a Kalman Filter based innovation model in state space representation.

3.3 Statistical Properties of the Performance Measure

[1]The performance index is evaluated by using the correlations between the white noise input a_t and the process output y_t. These correlation coefficients are directly proportional to the impulse response coefficients in Equation 3.2. Söderström and Stoica (1989) have shown that the estimated impulse response coefficients $\hat{f}_k$ have the following asymptotic statistical properties:

$$\hat{f}_k = \frac{\hat{\gamma}_{ya}(k)}{\hat{\sigma}_a^2} \overset{N \to \infty}{=} f_k \tag{3.10}$$

where $\hat{\gamma}_{ya}(k)$ and $\hat{\sigma}_a^2$ are the sample covariance and sample variance respectively. They have also shown that

$$E[(\hat{f}_\mu - f_\mu)(\hat{f}_\nu - f_\nu)] \simeq \frac{1}{N}[\sum_{i=0}^{\infty} f_i f_{i+|\nu-\mu|} + \sum_{\tau=-\mu}^{\nu} f_{\tau+\mu} f_{\nu-\tau} - 2 f_\mu f_\nu] \tag{3.11}$$

These results are useful in deducing the statistical properties of the performance index.

From Equation 3.3, the impulse response coefficient can be expressed as

$$f_k = \frac{\gamma_{ya}(k)}{\sigma_a^2} = \frac{\sigma_y}{\sigma_a} \frac{\gamma_{ya}(k)}{\sigma_y \sigma_a} = \frac{\sigma_y}{\sigma_a} \rho_{ya}(k) \tag{3.12}$$

If the sample size N is large, $\hat{\sigma}_y$ and $\hat{\sigma}_a$ are approximately equal to σ_y and σ_a respectively. Thus, the sampled version of the above equation is

$$\hat{f}_k = \frac{\hat{\sigma}_y}{\hat{\sigma}_a} \hat{\rho}_{ya}(k) \simeq \frac{\sigma_y}{\sigma_a} \hat{\rho}_{ya}(k) \tag{3.13}$$

---

[1]This section is adapted from an internal report titled "Control Loop Performance Assessment of SISO Processes" of Huang (1995).

Substituting this relationship into the left hand side of Equation 3.11 yields

$$E[(\widehat{\rho}_{ya}(\mu) - \rho_{ya}(\mu))(\widehat{\rho}_{ya}(\nu) - \rho_{ya}(\nu))] \simeq \frac{1}{N} \frac{\sigma_a^2}{\sigma_y^2} [\sum_{i=0}^{\infty} f_i f_{i+|\nu-\mu|} + \sum_{\tau=-\mu}^{\nu} f_{\tau+\mu} f_{\nu-\tau} - 2 f_\mu f_\nu]$$

(3.14)

On the other hand, the autocovariance of y_t is

$$\gamma_y(\mu - \nu) = E[y_\mu y_\nu] = \sigma_a^2 \sum_{i=0}^{\infty} f_i f_{i+|\nu-\mu|}$$

(3.15)

Therefore,

$$\sum_{i=0}^{\infty} f_i f_{i+|\nu-\mu|} = \frac{\gamma_y(\mu - \nu)}{\sigma_a^2} = \frac{\sigma_y^2}{\sigma_a^2} \rho_y(\mu - \nu)$$

(3.16)

Substituting Equation 3.12 and Equation 3.16 into the right hand side of Equation 3.14 gives the covariance of the estimated correlation $P_{\mu\nu}$, that is,

$$P_{\mu\nu} \triangleq E[(\widehat{\rho}_{ya}(\mu) - \rho_{ya}(\mu))(\widehat{\rho}_{ya}(\nu) - \rho_{ya}(\nu))]$$

$$\simeq \frac{1}{N}[\rho_y(\mu - \nu) + \sum_{\tau=-\mu}^{\nu} \rho_{ya}(\tau + \mu)\rho_{ya}(\nu - \tau) - 2\rho_{ya}(\mu)\rho_{ya}(\nu)] \quad (3.17)$$

With the covariance of the estimated correlation available, the second moment of the performance index $\widehat{\eta}(d) = \widehat{X}^T \widehat{X}$ can be approximated by its first order Taylor Series (Wolter, 1985) expansion as

$$mse(\widehat{\eta}(d)) = E[\widehat{X}^T \widehat{X} - X^T X]^2 \simeq l^T \Sigma l$$

(3.18)

where

$$l = \frac{\partial(\widehat{X}^T \widehat{X})}{\partial \widehat{X}}|_{\widehat{X}=X} = 2X$$

(3.19)

$$\Sigma = COV(\widehat{X}) = [P_{\mu\nu}]$$

$$= \begin{bmatrix} P_{0,0} & P_{0,1} & \cdots & P_{0,d-1} \\ P_{1,0} & P_{1,1} & \cdots & P_{1,d-1} \\ \vdots & \vdots & \ddots & \vdots \\ P_{d-1,0} & P_{d-1,1} & \cdots & P_{d-1,d-1} \end{bmatrix}$$

(3.20)

In practice, the population values can be substituted by their corresponding sample quantities. This gives

$$mse(\widehat{\eta}(d)) \simeq \widehat{l}^T \widehat{\Sigma} \widehat{l} = 4 \widehat{X}^T \widehat{\Sigma} \widehat{X}$$

(3.21)

34

where

$$\widehat{\Sigma} = [\widehat{P}_{\mu\nu}] \qquad (3.22)$$

and each element of $\widehat{\Sigma}$ is given by:

$$\widehat{P}_{\mu\nu} = \frac{1}{N}[\widehat{p}_y(\mu - \nu) + \sum_{\tau=-\mu}^{\nu} \widehat{p}_{ya}(\tau + \mu)\widehat{p}_{ya}(\nu - \tau) - 2\widehat{p}_{ya}(\mu)\widehat{p}_{ya}(\nu)] \qquad (3.23)$$

With Equation 3.21, it is convenient to calculate the confidence level of the feedback performance measure. For instance, the 95% confidence bounds of the measure is $\pm 2\sqrt{mse(\widehat{\eta}(d))}$. The *Matlab* code for calculating the performance measure and the confidence bounds is provided in Appendix A.

3.4 Industrial Application

The NO_2 production process studied in the previous chapter is utilized again to demonstrate the technique of control loop performance assessment. The simplified schematic and instrument diagram of the catalytic reactor is shown in Figure 3.2.

The catalyst temperature of the reactor (T106) is controlled by a PID controller (TC3) which is cascaded to the ammonia flow controller (FC3). The sampling rate of the process is 10 seconds, and the process time delay is approximately 2 sampling periods. A plot of the catalyst temperature collected over a one-day period is illustrated in Figure 3.3.

It can be seen from Figure 3.3 that the process data is noisy. In order to determine whether the output variance can be reduced by retuning the feedback controller, the performance of the outer loop of the catalyst temperature control is assessed by estimating the feedback controller performance index as defined in Equation 3.5. By applying the FCOR algorithm to a window of 1000 process data points, the performance index and its 95% confidence bounds are calculated and plotted in Figure 3.4. The small values of the index, with an average of 0.161±0.067, indicate poor performance of the catalyst temperature control loop. The sudden drop of performance index during the sampling periods from 1000 to 2000, 3000 to 4000 and 6000
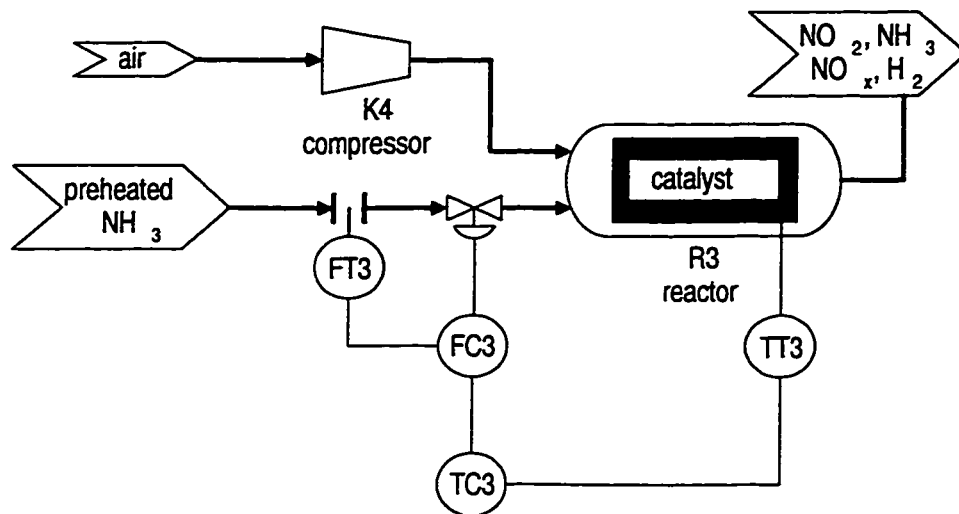
Figure 3.2: Simplified schematic and instrument diagram of the catalytic reactor control loop.
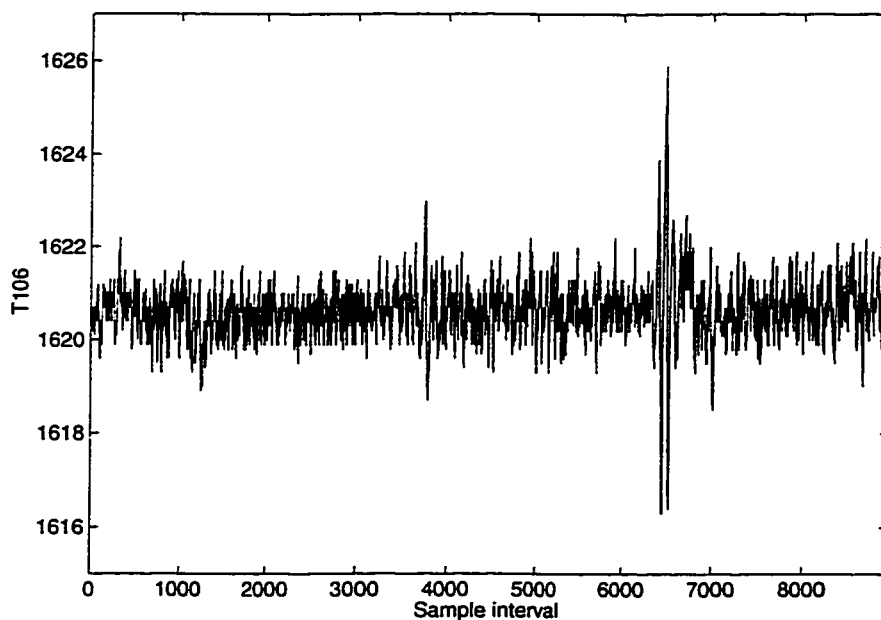
Figure 3.3: Time plot of the catalyst temperature.

36
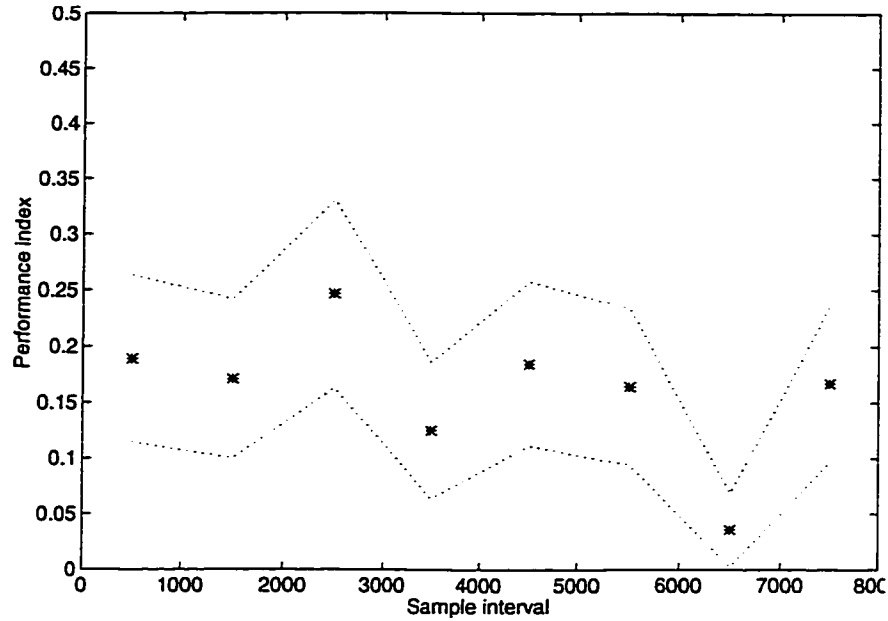
Figure 3.4: Performance of the outer loop of the cascade reactor control with 95% confidence bounds.

to 7000 show that changes might have occurred in the system. It can be observed from the time plot in Figure 3.3 that large process variations have erupted during these periods. Further diagnosis of the process reveals that disturbances enter the system through the temperature changes of the superheated ammonia and ambient air. In this example, the control loop performance can be improved by retuning the controller. If the disturbances can be measured on-line, they could be corrected by feedforward control. The method to evaluate the feasibility of the addition of feedforward control to an existing feedback control system will be discussed in the next chapter.

3.5 Conclusions

The performance of an existing control loop is often measured against some benchmarks. There are many different measures of control performance, and the minimum

variance control benchmark is one of the most popular. The feedback control loop performance index defined by Huang (1997) is studied in this chapter. The FCOR algorithm, as well as the statistical properties of the index, is also discussed, and applied to an industrial NO_2 production process.

Chapter 4

Payout Measure for Implementing Feedforward Control

4.1 Introduction

Feedback control is a widely used control strategy in process industries due to its simplicity of use and implementation. It requires little information about the source or type of disturbance in the system, and corrective action occurs only when the controlled variable deviates from the setpoint. This, however, also means that feedback control is not able to provide predictive control action to compensate for the effects of measurable disturbances and causes the process to suffer from frequent disturbances. This kind of controller performance may not be acceptable in some cases, and hence other control schemes should be considered to improve it.

With feedforward control, measurable disturbances are compensated for before they upset the process. This control scheme is worth implementing only when the time delay exists and the measurable disturbances significantly affect the system response. Therefore, it is important to have an efficient and effective tool to evaluate the "payout" for implementing a feedforward controller into an existing feedback control loop.

In this chapter, a "payout" measure is introduced for the case of stochastic mea-
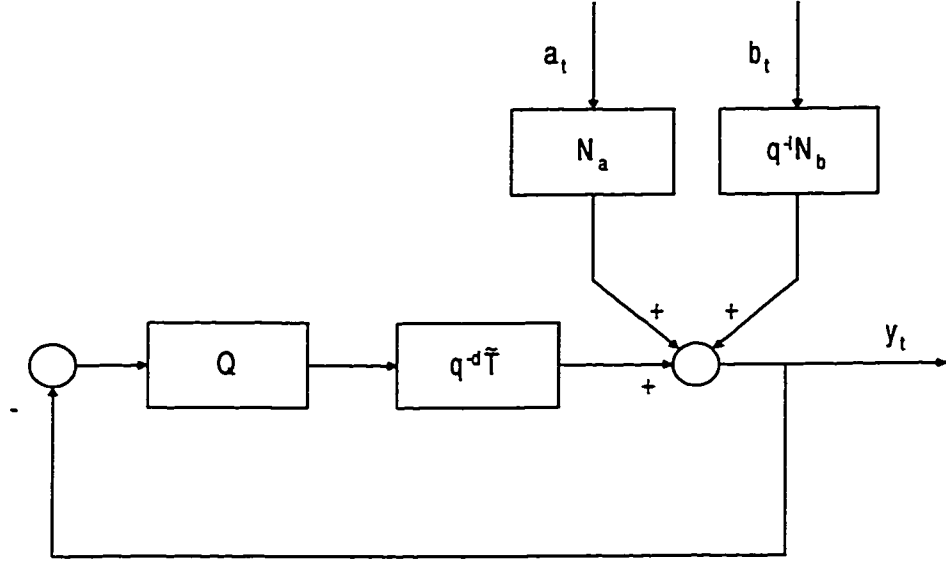
Figure 4.1: Block diagram of a closed-loop system with two disturbances.

surable disturbance. The performance prediction of a feedback plus feedforward control system is also discussed. Simulation, experimental and industrial examples are presented to illustrate the application of the analysis.

4.2 Payout Measure of Feedforward Control

The closed-loop system in Figure 1.1 is modified such that the process is influenced by two types of disturbances: measurable and unmeasurable. The block diagram of this new system is depicted in Figure 4.1. The output response of the process is

$$y_t = \frac{N_a}{1 + q^{-d}Q\widetilde{T}}a_t + \frac{q^{-l}N_b}{1 + q^{-d}Q\widetilde{T}}b_t \qquad (4.1)$$

where a_t and b_t are the driving forces of the unmeasurable and measurable disturbances respectively, N_a and N_b are the load models, and l is the time delay of the measurable load. Both a_t and b_t are sequences of zero mean. They are independently and identically distributed random variates.

Long division yields a sum of two infinite impulse responses, that is,

$$y_t = (f_{a,0} + f_{a,1}q^{-1} + \cdots + f_{a,d-1}q^{-d+1} + f_{a,d}q^{-d} + \cdots)a_t + \qquad (4.2)$$

$$(f_{b,0} + f_{b,1}q^{-1} + \cdots + f_{b,d-1}q^{-d+1} + f_{b,d}q^{-d} + \cdots)b_t$$

where $f_{a,j}$ and $f_{b,j}$ for $j = 0, 1, 2, \ldots$ are the impulse response coefficients of y_t observed from a_t and b_t respectively. Since a_t and b_t are independent and uncorrelated, multiplying Equation 4.2 by $a_t, a_{t-1}, \ldots, b_t, b_{t-1}, \ldots$ respectively and then taking statistical expectation yields the cross covariance coefficients

$$\gamma_{ya}(0) = E[y_t a_t] = f_{a,0}\sigma_a^2$$

$$\gamma_{ya}(1) = E[y_t a_{t-1}] = f_{a,1}\sigma_a^2$$

$$\vdots$$

$$\gamma_{yb}(0) = E[y_t b_t] = f_{b,0}\sigma_b^2$$

$$\gamma_{yb}(1) = E[y_t b_{t-1}] = f_{b,1}\sigma_b^2$$

$$\vdots \qquad (4.3)$$

Therefore, the variance of y_t is

$$\sigma_y^2 = (f_{a,0}^2 + f_{a,1}^2 + \cdots + f_{a,d-1}^2 + f_{a,d}^2 + \cdots)\sigma_a^2 +$$

$$(f_{b,0}^2 + f_{b,1}^2 + \cdots + f_{b,d-1}^2 + f_{b,d}^2 + \cdots)\sigma_b^2$$

$$= \sigma_{ya}^2 + \sigma_{yb}^2 \qquad (4.4)$$

where σ_a^2 and σ_b^2 are the variances of the driving forces a_t and b_t. The first term of Equation 4.4, σ_{ya}^2, is the variance contribution by the unmeasurable disturbance to the total output variance, and the second term, σ_{yb}^2, is the variance contribution by the measurable disturbance to the total output variance.

The payout measure of feedforward control relative to the total output variance is defined as

$$\eta_{FF} = \frac{(f_{b,0}^2 + f_{b,1}^2 + \cdots + f_{b,d-1}^2 + f_{b,d}^2 + \cdots)\sigma_b^2}{\sigma_y^2}$$

$$= \frac{\sigma_{yb}^2}{\sigma_y^2} \qquad (4.5)$$

This is simply to obtain a measure of the contribution of the measurable disturbance towards the total output variance. Since the variance contribution of b_t cannot be greater than the total output variance, η_{FF} must always be less than one, or $0 \leq \eta_{FF} \leq 1$. Unlike the feedback controller performance index $\eta(d)$, η_{FF} is not a function of the process delay d. Substituting the results from Equation 4.3 into the above equation gives

$$
\begin{aligned}
\eta_{FF} &= \frac{\gamma_{b,0}^2 + \gamma_{b,1}^2 + \cdots + \gamma_{b,d-1}^2 + \gamma_{b,d}^2 + \cdots}{\sigma_y^2 \sigma_b^2} \\
&= \rho_{yb}^2(0) + \rho_{yb}^2(1) + \cdots \rho_{yb}^2(d-1) + \rho_{yb}^2(d) + \cdots
\end{aligned}
\tag{4.6}
$$

where $\rho_{yb}(0)$, $\rho_{yb}(1)$, ... are the cross correlation coefficients between y_t and b_t. The sampled version of this payout measure is

$$
\widehat{\eta}_{FF} = \widehat{\rho}_{yb}^2(0) + \widehat{\rho}_{yb}^2(1) + \cdots + \widehat{\rho}_{yb}^2(d-1) + \widehat{\rho}_{yb}^2(d) + \cdots
\tag{4.7}
$$

where

$$
\widehat{\rho}_{yb}(k) = \frac{\frac{1}{N} \sum_{t=k+1}^{N} y_t b_{t-k}}{\sqrt{\frac{1}{N} \sum_{t=1}^{N} y_t^2 \frac{1}{N} \sum_{t=1}^{N} b_t^2}}
\tag{4.8}
$$

In practice, the infinite summation in Equation 4.7 is truncated when additional terms no longer make significant contribution to the measure. Since both y_t and b_t are known, their correlation can easily be evaluated from routine closed-loop data.

This payout measure can be used to evaluate the significance of b_t to the process. When the measure is large, it indicates that b_t has a significant contribution to the total output variance σ_y^2; and hence, most of the process variability can be eliminated by removing b_t before it upsets the process. Therefore, implementing feedforward control is potentially effective in reducing the process variability in this case. For instance, if $\eta_{FF} > 0.5$, it means that more than half of the total variance is induced by b_t. A perfect feedforward controller if implemented, which is only possible when $l \geq d$, will result in a reduction of at least half of the total output variance. On the other hand, if η_{FF} is small (e.g. $\eta_{FF} = 0.1$), the process variance is mainly contributed by other disturbances besides b_t. Adding a feedforward controller in this case to correct b_t will not reduce the output variance very much.

Although this payout measure can be used to predict how well a perfect feedforward controller would perform, the decision of whether to implement the feedforward control scheme still depends on the cut-off index. That is, a payout measure of $\eta_{FF} = 0.3$, or 33 percent potential reduction of the process variance, does not necessarily mean that adding feedforward control is economically unattractive. For example, too low a catalyst temperature of a reactor would promote the yield of undesired by-products, whereas too high would cause premature catalyst degradation. This limits a narrow temperature operation range (e.g. $\Delta T \pm 5°F$). In this type of situation, a small reduction of temperature variance would help maintain the catalyst temperature within the narrow operating band, improving product yield and increasing the life of catalyst. In some other cases, even a payout measure $\eta_{FF} = 0.7$ would not justify the implementation of a feedforward controller. Therefore, there is no well-defined threshold for this payout measure.

4.3   Performance Prediction of Feedback plus Feedforward Control

The payout measure indicates only the feasibility of incorporating feedforward control to an existing feedback control loop. However, it is also of great interest to know how the future feedback plus feedforward controller is going to perform beforehand. The index introduced in this section predicts the performance of the future feedback plus feedforward control without the need to actually implement the feedforward controller. Two cases are investigated: (i) the measurable disturbance delay is greater than the process delay $l \geq d$; and (ii) the process delay is greater than the disturbance delay $d > l$.

Case (i) $l \geq d$

Whenever l is greater than or equal to d, it is possible to design a perfect feedforward controller to completely eliminate b_t. Consider the system in Figure 4.1 and

Equation 4.2 again. Equation 4.2 can also be expressed as

$$
y_t = \underbrace{(f_{a,0} + f_{a,1}q^{-1} + \cdots + f_{a,d-1}q^{-(d-1)})a_t}_{y_{a,mv}} + \underbrace{(f_{a,d}q^{-d} + f_{a,d+1}q^{-(d+1)} + \cdots)a_t}_{y_{a,non\_mv}} +
$$
$$
\underbrace{(f_{b,0} + f_{b,1}q^{-1} + \cdots + f_{b,d-1}q^{-(d-1)})b_t}_{y_{b,mv}} +
$$
$$
\underbrace{(f_{b,d}q^{-d} + \cdots + f_{b,l-1}q^{-(l-1)})b_t}_{y_{b,FF1}} + \underbrace{(f_{b,l}q^{-l} + \cdots + f_{b,l+1}q^{-(l+d-1)})b_t}_{y_{b,FF2}} +
$$
$$
\underbrace{(f_{b,l+d}q^{-(l+d)} + f_{b,l+d+1}q^{-(l+d+1)} + \cdots)b_t}_{y_{b,non\_mv}} \tag{4.9}
$$

which consists of contributions from a_t and b_t. $y_{a,mv}$ is the contribution to minimum variance from a_t, whereas y_{a,non_mv} is due to the non-optimality of the feedback controller. $y_{b,mv}$ is the contribution to minimum variance from b_t. $y_{b,FF} = y_{b,FF1} + y_{b,FF2}$ is due to the non optimality of the feedforward controller, and y_{b,non_mv} is due to the non optimality of the feedback and/or feedforward controller. Since $l \geq d$, the first l terms of the contribution from b_t should be zero, or simply $y_{b,mv}$ and $y_{b,FF1}$ are zero. The fifth term, $y_{b,FF2}$, could also be labelled as the feedback invariant term. However it can be eliminated by perfect feedforward control when $l \geqslant d$. Equation 4.9 is then reduced to:

$$
y_t = \underbrace{(f_{a,0} + f_{a,1}q^{-1} + \cdots + f_{a,d-1}q^{-(d-1)})a_t}_{y_{a,mv}} + \underbrace{(f_{a,d}q^{-d} + f_{a,d+1}q^{-(d+1)} + \cdots)a_t}_{y_{a,non\_mv}} +
$$
$$
\underbrace{(f_{b,l}q^{-l} + f_{b,l+1}q^{-(l+1)} + \cdots + f_{b,l+1}q^{-(l+d-1)})b_t}_{y_{b,FF2}} +
$$
$$
\underbrace{(f_{b,l+d}q^{-(l+d)} + f_{b,l+d+1}q^{-(l+d+1)} + \cdots)b_t}_{y_{b,non\_mv}} \tag{4.10}
$$

It is important to notice that $\sigma^2_{yb,mv}$ is zero not due to correction from any kind of feedforward controller but simply because of the nature of the process ($l \geq d$).

Assume that all the effect of the measurable disturbance is removed by a perfect feedforward controller. That means $y_{b,FF2}$ and y_{b,non_mv} are eliminated. Then the new process variance will be induced solely from the unmeasurable disturbance; that is,

$$
\sigma^2_{y(FB+FF)} = Var[y_{a,mv} + y_{a,non\_mv}]
$$

$$= (f_{a,0}^2 + f_{a,1}^2 + \cdots + f_{a,d-1}^2 + f_{a,d}^2 + \cdots)\sigma_a^2$$

$$= \sigma_{ya}^2 \tag{4.11}$$

Therefore, the performance of the feedback controller with feedforward compensation, using minimum variance feedback plus feedforward controller as benchmark, is given by

$$
\begin{aligned}
\eta_{FB+FF}(d) &= \frac{Var[y_{a,mv}]}{Var[y_{a,mv} + y_{a,non\_mv}]} \\
&= \frac{(f_{a,0}^2 + f_{a,1}^2 + \cdots + f_{a,d-1}^2)\sigma_a^2}{(f_{a,0}^2 + f_{a,1}^2 + \cdots + f_{a,d-1}^2 + f_{a,d}^2 + \cdots)\sigma_a^2} \\
&= \frac{f_{a,0}^2 + f_{a,1}^2 + \cdots + f_{a,d-1}^2}{f_{a,0}^2 + f_{a,1}^2 + \cdots + f_{a,d-1}^2 + f_{a,d}^2 + \cdots} \\
&= \frac{\sigma_{ya,mv}^2}{\sigma_{ya}^2} \tag{4.12}
\end{aligned}
$$

Here, η_{FB+FF} is again bounded by $[0,1]$. This index indicates how close to minimum variance will the feedback controller be operating with the correction from a perfect feedforward controller. If the feedback controller is close to minimum variance, $\sigma_{ya}^2 \simeq \sigma_{ya,mv}^2$ and hence η_{FB+FF} will be close to one. Retuning of the feedback controller will not provide any reduction of the output variance. On the other hand if η_{FB+FF} is small or close to zero, the feedback controller should be retuned in order to further reduce the output variance.

Without feedforward control, the performance of the feedback only controller measured against the minimum variance feedback plus feedforward controller would be

$$
\begin{aligned}
\eta_{FB+FF}^*(d) &= \frac{Var[y_{a,mv}]}{\sigma_y^2} \\
&= \frac{(f_{a,0}^2 + f_{a,1}^2 + \cdots + f_{a,d-1}^2)\sigma_a^2}{\sigma_y^2} \\
&= \frac{\sigma_{ya,mv}^2}{\sigma_y^2} \tag{4.13}
\end{aligned}
$$

Considering $\sigma_y^2 > \sigma_{ya}^2$, η_{FB+FF} must indicate better controller performance than η_{FB+FF}^*. The difference between their values indicates the best potential improvement in the controller performance by incorporating feedforward control to the existing

feedback control loop. The larger the difference, the greater the benefit from the feedforward controller.

Since $\sigma_{ya,mv}^2$ and σ_{ya}^2 cannot be obtained directly from process measurement, they have to be estimated via identification of the closed-loop transfer functions of Equation 4.1. The procedure for evaluating η_{FB+FF} is as follows:

1. Identify the closed-loop transfer functions in Equation 4.1 by time series models such as ARMAX or Box-Jenkins models.

2. Calculate the impulse response coefficients $f_{a,0}$, $f_{a,1}$, ..., and $f_{b,0}$, $f_{b,1}$, ... by deconvolving $1 + q^{-d}QT$ out of N_a and N_b respectively.

3. Calculate η_{FB+FF} using Equation 4.12.

Case (ii) $d > l$

If the process delay d is greater than the load delay l, the output of the process in Figure 4.1 will be

$$
y_t = \underbrace{(f_{a,0} + f_{a,1}q^{-1} + \cdots + f_{a,d-1}q^{-(d-1)})a_t}_{y_{a,mv}} + \underbrace{(f_{a,d}q^{-d} + f_{a,d+1}q^{-(d+1)} + \cdots)a_t}_{y_{a,non\_mv}} +
$$

$$
\underbrace{(f_{b,0} + f_{b,1}q^{-1} + \cdots + f_{b,l-1}q^{-(l-1)} + f_{b,l}q^{-l} + \cdots + f_{b,d-1}q^{-(d-1)})b_t}_{y_{b,mv}} +
$$

$$
\underbrace{(f_{b,d}q^{-d} + \cdots + f_{b,l+1}q^{-(l+d-1)})b_t}_{y_{b,FF}} +
$$

$$
\underbrace{(f_{b,l+d}q^{-(l+d)} + f_{b,l+d+1}q^{-(l+d+1)} + \cdots)b_t}_{y_{b,non\_mv}} \tag{4.14}
$$

The first l terms in $y_{b,mv}$ are zero and Equation 4.14 is reduced to

$$
y_t = \underbrace{(f_{a,0} + f_{a,1}q^{-1} + \cdots + f_{a,d-1}q^{-(d-1)})a_t}_{y_{a,mv}} + \underbrace{(f_{a,d}q^{-d} + f_{a,d+1}q^{-(d+1)} + \cdots)a_t}_{y_{a,non\_mv}} +
$$

$$
\underbrace{(f_{b,l}q^{-l} + \cdots + f_{b,d-1}q^{-(d-1)})b_t}_{y_{b,mv}} + \underbrace{(f_{b,d}q^{-d} + \cdots + f_{b,l+1}q^{-(l+d-1)})b_t}_{y_{b,FF}} +
$$

$$
\underbrace{(f_{b,l+d}q^{-(l+d)} + f_{b,l+d+1}q^{-(l+d+1)} + \cdots)b_t}_{y_{b,non\_mv}} \tag{4.15}
$$

Since a perfect feedforward controller is not physically realizable when $d > l$, a static feedforward control, which will not be able to totally eliminate b_t, has to be considered. In this case, the index introduced in Equation 4.12, which is formulated based on the assumption of complete removal of b_t, is no longer valid. Hence, it is impossible to predict how much of b_t can the future feedforward controller remove from the process. The only information that can be obtained is the performance of the feedback only controller compared to the minimum variance feedback plus feedforward controller. Note, since only the first l terms of the impulse response expression are zero, $\sigma^2_{yb,mv}$ is no longer zero for processes with $d > l$. As a result, the performance measure is

$$
\begin{aligned}
\eta^*_{FB+FF}(d) &= \frac{Var[y_{a,mv} + y_{b,mv}]}{\sigma^2_y} \\
&= \frac{(f^2_{a,0} + f^2_{a,1} + \cdots + f^2_{a,d-1})\sigma^2_a + (f^2_{b,l} + f^2_{b,l+1} + \cdots + f^2_{b,d-1})\sigma^2_b}{\sigma^2_y} \\
&= \frac{\sigma^2_{ya,mv} + \sigma^2_{yb,mv}}{\sigma^2_y}
\end{aligned}
\tag{4.16}
$$

This index also becomes the lower performance bound for the future feedback plus feedforward control loop when the static feedforward controller is unable to reduce the effect of b_t at all. If at least part of b_t is corrected, σ^2_y will be smaller and hence η^*_{FB+FF} will be a step closer to the best achievable performance.

Note that the above index is different from Huang's SISO feedback performance index. Recall the feedback performance index evaluated using FCOR algorithm in the previous chapter, denoted as $\eta_{FB}(d)$ here in this chapter, is calculated by filtering the lumped disturbance z_t from the process output y_t; that is

$$
\begin{aligned}
\eta_{FB}(d) &= \frac{(f^2_{z,0} + f^2_{z,1} + \cdots + f^2_{z,d-1})\sigma^2_z}{\sigma^2_y} \\
&= \rho^2_{yz}(0) + \rho^2_{yz}(1) + \cdots \rho^2_{yz}(d-1)
\end{aligned}
\tag{4.17}
$$

where z_t is the lumped disturbance of a_t and b_t. In a situation where measurable and unmeasurable disturbances can be distinguished from each other, Equation 4.16 provides performance evaluation against the minimum variance feedforward plus feedback control.

4.4 Simulation Study

Performance assessment analysis as discussed in the previous sections is illustrated on a simple process with a proportional and integral (PI) feedback controller. The process is first order with a time delay of 3 sampling periods as shown in Figure 4.2. In this case, the measurable load has a delay of 5 sampling periods. The driving forces of the unmeasurable and measurable disturbances, a_t and b_t respectively, are sequences of independent random noises with mean zero. The effect of the variance of these noises on the performance index of the PI controller is investigated.

Five simulation runs were performed with the noise variance σ_a^2 changed. The variance of the disturbances and their contribution on the output variance are listed in Table 4.1. Table 4.2 summarizes the performance of the feedback only controller, and the feedback plus feedforward controller measured against the minimum variance feedback plus feedforward controller, η^*_{FB+FF} and η_{FB+FF} respectively, for the various cases. The same table also provides the payout measure η_{FF} and the percentage improvement in performance based on the difference between the values of the feedback only and feedback plus feedforward control measures.

Assume that the threshold for implementing feedforward control of this process is $\eta_{FF} = 0.5$; this means that feedforward control should be employed whenever b_t contributes more than half of the total variance. In cases (i), (ii) and (iii) of Table 4.2, η_{FF} is greater than 0.5. Especially in case (i) where $\eta_{FF} = 0.935$, more than 90% of the output variance originated from b_t. All these three cases have a performance improvement over 100 percent of the original feedback only control loop performance. Therefore, adding feedforward control to the existing feedback system is recommended. On the other hand, both cases (iv) and (v) have η_{FF} less than 0.5. Their percentage performance improvement are 45.9 and 25.8 percent respectively. This indicates that it may not be useful to implement feedforward control to reduce the output variance.
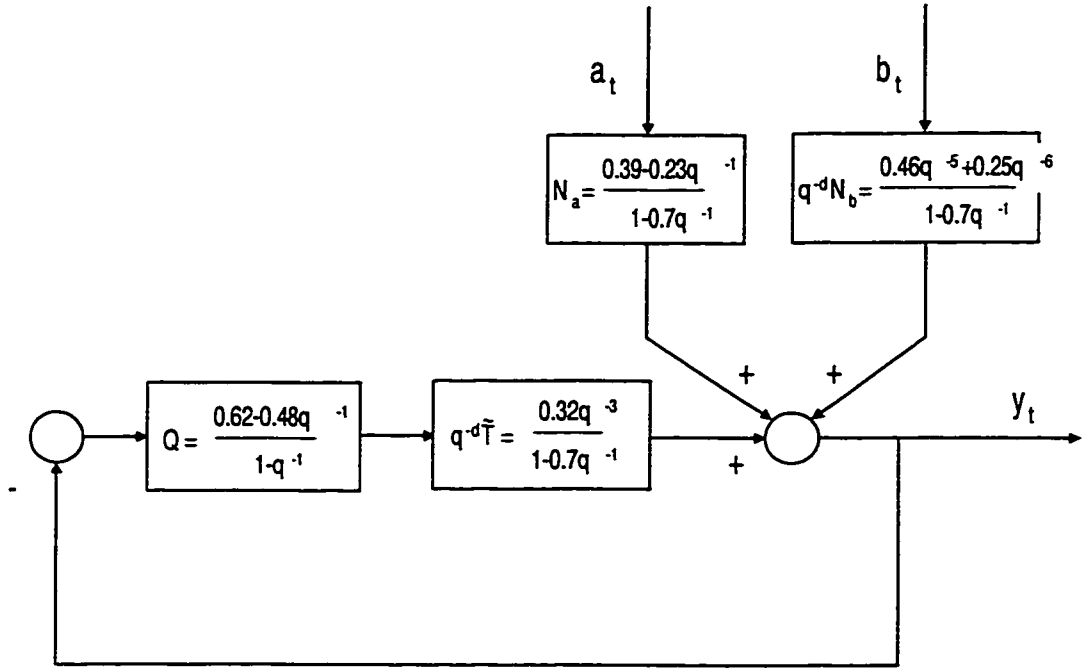
Figure 4.2: Block diagram of a closed-loop system used for simulation study.

Table 4.1: Analysis of variance of the simulated process.

Case	Disturbance variance		Minimum variance		Contribution of disturbance		Output variance
	σ_a^2	σ_b^2	$\sigma_{a,mv}^2$	$\sigma_{b,mv}^2$	σ_{ya}^2	σ_{yb}^2	σ_y^2
i	0.25	1.44	0.113	0	0.231	1.30	1.39
ii	1.00	1.00	0.252	0	0.285	0.883	1.10
iii	2.25	0.64	0.348	0	0.389	0.589	0.970
iv	4.00	0.36	0.616	0	0.691	0.328	1.01
v	4.48	0.25	0.745	0	0.836	0.226	1.05

Table 4.2: Control performance of the simulated process.

Case	FF payout measure η_{FF}	FB only performance η^*_{FB+FF}	FB+FF performance η_{FB+FF}	Performance improvement $\frac{\eta_{FB+FF}-\eta^*_{FB+FF}}{\eta^*_{FB+FF}} \times 100\%$
i	0.935	0.0813	0.488	501
ii	0.806	0.230	0.886	285
iii	0.608	0.358	0.893	149
iv	0.325	0.611	0.892	45.9
v	0.215	0.709	0.891	25.8

4.5 Experimental Application

In this section, evaluation of the performance assessment technique is illustrated on a pilot scale process, as presented schematically in Figure 4.3.

In this experiment, cold water and warm water enter the glass tank 1 through control valves 1 (CV1) and 3 (CV3) respectively. The water inside tank 1 is heated by steam. The heated water then flows out through a long copper tube. Thermocouples are located at various distances from tank 1 along the tube to tank 2 for drainage. The objective of this experiment is to control the water temperature of tank 1, measured via thermocouple 2 (TT2), by manipulating the steam valve (CV2) position. A PI controller is implemented on a real-time sensor based computer system through Matlab and Simulink with a sampling time of 5 seconds. Signals are exchanged via an OPTO 22 I/O subsystem. The water level is controlled automatically by a Fisher DPR900 PI controller. The level setpoint is tracked by manipulating CV1.

An artificially generated random noise signal was injected into CV3 to create a source of unmeasurable stochastic disturbance. The water level setpoint was stepped up and down to produce a series of measurable disturbances.

One of the most important piece of information about the process required for performance assessment is the time delay of the process and the measurable distur-
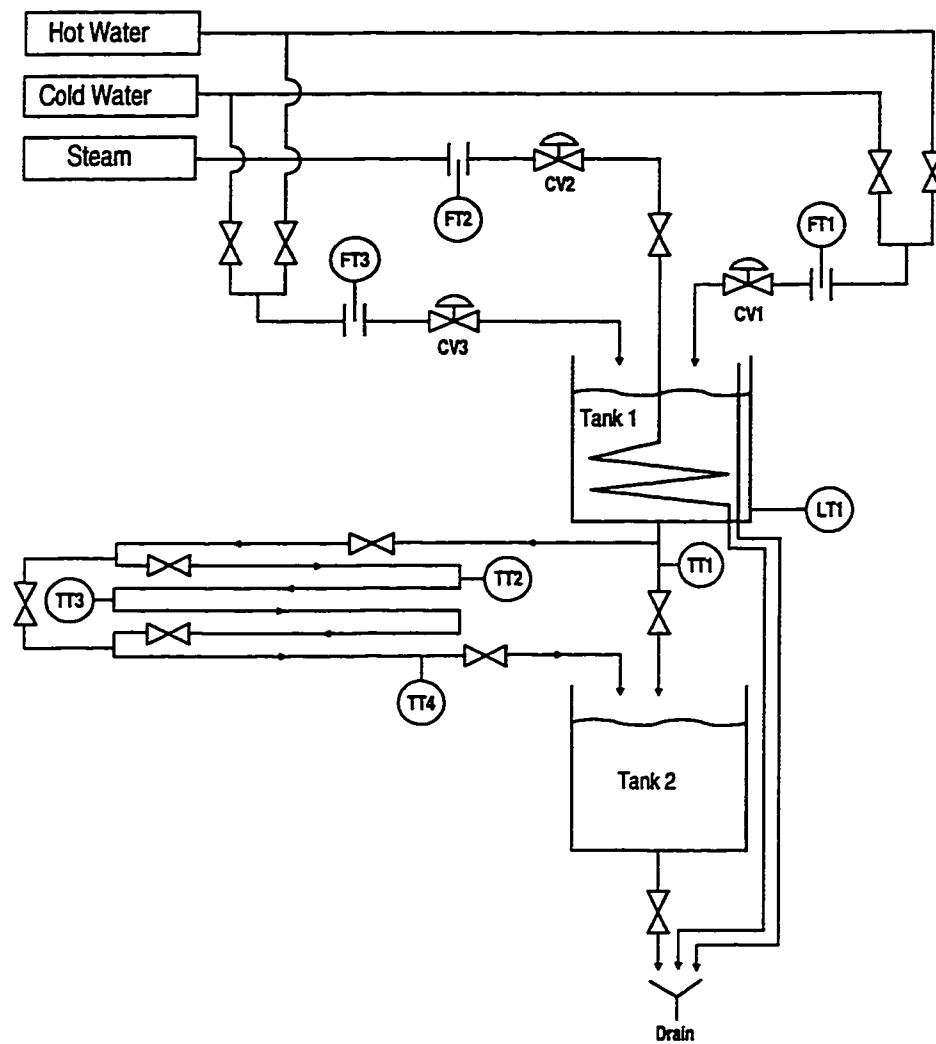
Figure 4.3: Schematic diagram of a pilot scale process.

Table 4.3: Analysis of variance of the pilot scale process.

Sample intervals	Disturbance variances		Minimum variances		Contribution of disturbances		Output variance
	σ_a^2	σ_b^2	$\sigma_{a,mv}^2$	$\sigma_{b,mv}^2$	σ_{ya}^2	σ_{yb}^2	σ_y^2
210 - 1000	0.0761	0.528	0.000473	0	0.00398	0.00140	0.00687
1010 - 2000	0.284	0.527	0.00189	0	0.0165	0.000498	0.0208
2010 - 3000	0.657	0.527	0.00387	0	0.0376	0.000629	0.0399

bance. Both the process delay and the measurable disturbance delay are determined to be 6 sample intervals through open loop bump tests.

Routine closed loop data were collected over 3000 sample intervals. These data are divided into three portions: 210 to 1000, 1010 to 2000 and 2010 to 3000 sample intervals. Performance assessment is applied individually to these three sets of data. The variance of the measurable disturbance remains approximately the same throughout the experiment while that of the unmeasurable disturbance increases from one portion to another. The output responses of the system is plotted in Figure 4.4.

The first step of the performance analysis is to evaluate the payout measure for feedforward control from the closed-loop data. After the closed-loop transfer function of the process is identified by an ARMAX model, the performance measures of the feedback only control and the feedback plus feedforward control are also calculated using Equations 4.12 and 4.13 respectively. The analysis of variance and the value of the performance measures are summarized in Tables 4.3 and 4.4 respectively.

As shown in Table 4.4, the payout measure for 210 to 1000 sample intervals is 0.204. This indicates that over 20 percent of the output variance is contributed by the measurable disturbance. Although the contribution looks small, comparison of η_{FB+FF}^* and η_{FB+FF} reveals that more than 70 percent of improvement over the feedback only control can be obtained if the measurable disturbance is eliminated by a perfectly-designed feedforward controller. Hence, it is worthwhile to implement feedforward control for this time period even though η_{FF} is not particularly large.
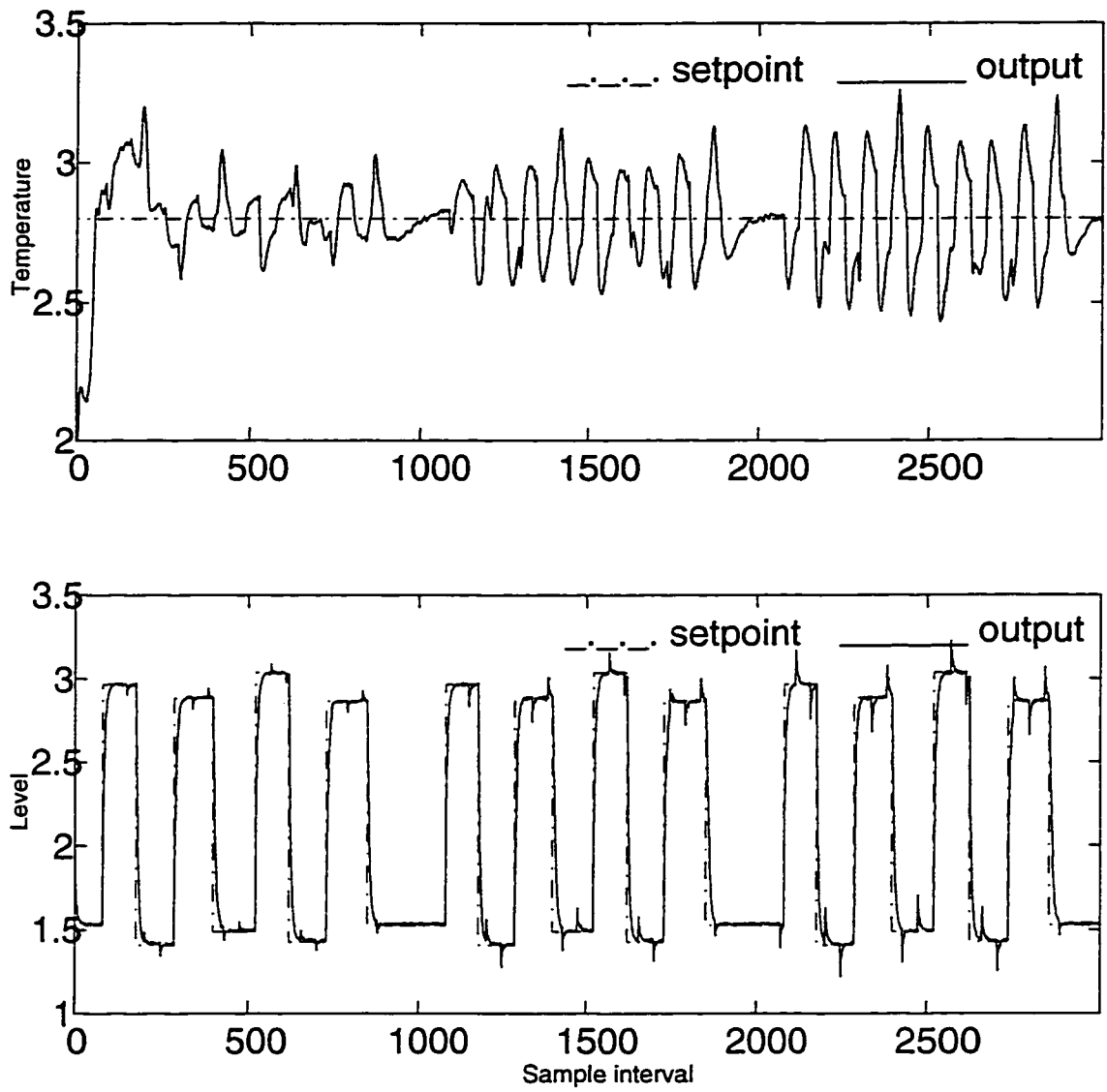
Figure 4.4: Output responses of the pilot scale process.

Table 4.4: Control performance of the pilot scale process.

Sample intervals	FF payout measure η_{FF}	FB only performance η^*_{FB+FF}	FB+FF performance η_{FB+FF}	Performance improvement $\frac{\eta_{FB+FF}-\eta^*_{FB+FF}}{\eta^*_{FB+FF}} \times 100\%$
210 - 1000	0.204	0.0689	0.119	72.7
1010 - 2000	0.0239	0.908	0.114	25.8
2010 - 3000	0.0158	0.970	0.103	6.05

The analysis also shows that feedforward control is not necessary for the last two portions as σ^2_a is increased to make the contribution of b_t to the output variance relatively smaller. Changes in level setpoint is not as significant to the process as changes in valve opening of CV3 to the water temperature in these two portions. The payout measure indicates that only 2.39 and 1.58 percent of the output variance is contributed by the measurable disturbance; that is, the level setpoint changes. The improvement in performance, a feedback plus feedforward controller can provide is also small (25.8 and 6.05 percent respectively). Therefore, feedforward control is not recommended in these two cases.

4.6 Industrial Application

In this section, performance analysis is applied to the industry example that has been discussed in the previous two chapters. A complete schematic and instrument diagram of the NO_2 production process, including the ammonia preheating section, is shown in Figure 4.5.

The main function of this process is to produce NO_2 which is used by subsequent processes to produce urea. Subcooled liquid ammonia enters E1 where it is heated to a saturated vapor by 50 psig process steam. A proportional, integral and derivative (PID) controller is used to regulate the pressure of the saturated ammonia. The saturated ammonia enters E2a, E2b and E2c and is heated to about $290°F$ by the
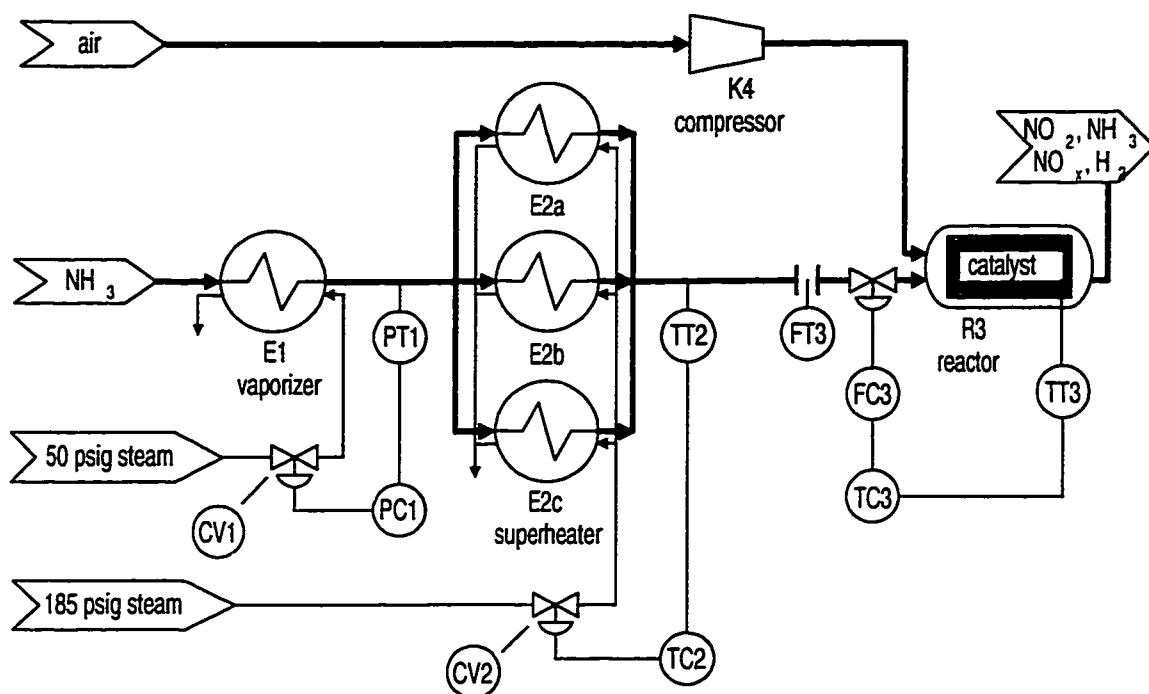
Figure 4.5: Simplified schematic and instrument diagram of the NO_2 production process.

185 psig process steam. The existing superheated ammonia temperature controller TC2 is also a PID controller. Superheated ammonia and compressed air enter the highly exothermic reactor R3, which produces NO_2 and NO_x in a yield of less than 50 percent. TC3 is a DMC controller which is cascaded to the ammonia flow controller FC3. All control loops are implemented on a Honeywell TDC2000 control system.

The operation of the catalytic reactor R3 is limited to a narrow range of catalyst temperature ($\pm 5^\circ F$). If the temperature drops too low, undesired by-products such as NO_x will be produced in significant quantities. If the temperature is too high, the catalyst will degrade prematurely. Control of the catalyst temperature is further complicated by disturbances to the ammonia temperature and the ambient air temperature. Heat exchangers E1 and E2 use process steam which has a significantly higher variance in pressure than utility steam. Although the pressure of the steam header is regulated, there are numerous disturbances caused by load changes in adjacent processes. Interactions between E2 and R3 result in additional disturbances to the ammonia temperature.

The objective of the analysis is to determine the benefits of implementing a feedforward controller to minimize the effect of the disturbance to the ammonia temperature (T212X) at the merged exit of E2 on the catalyst temperature (T106). The sampling time is 10 seconds. Both the process delay and the load delay are two sampling periods. Time plots of the catalyst and the ammonia temperatures are provided in Figure 4.6. The process variation composes of continuous stochastic noise and some infrequent fluctuations. It can be observed that these fluctuations strongly affect the catalyst temperature, especially during the period from 6300 to 6700 sample intervals. Performance analysis is applied to the data at different time intervals to determine the effect of the variation in the ammonia temperature to the catalyst temperature. The results are tabulated in Table 4.5.

The low payout measure during the periods from 1200 to 3500 and 4000 to 6200 sample intervals reflects that the background stochastic noise in the ammonia temperature does not affect the catalyst temperature very much. This noise contributes
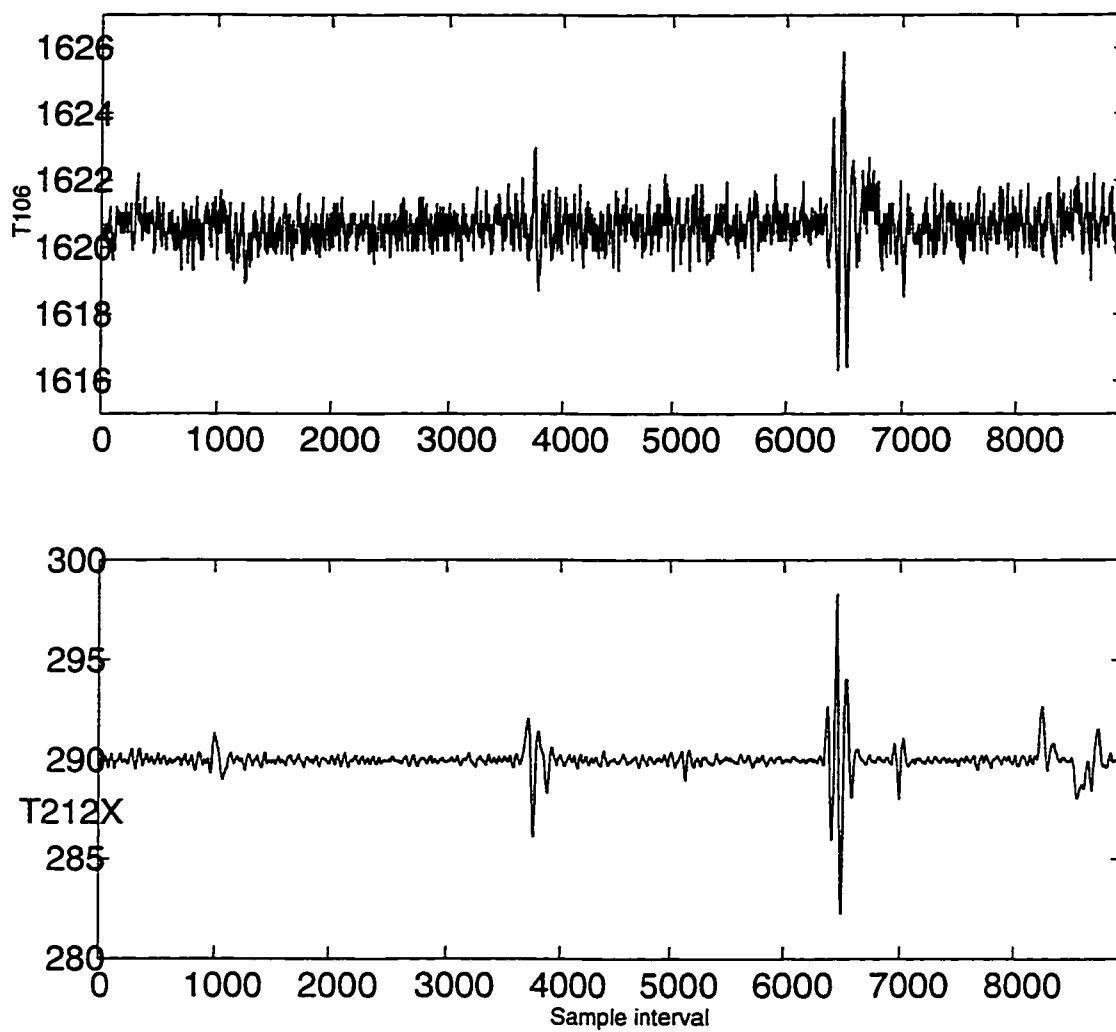
Figure 4.6: Time plots of the catalyst and the ammonia temperatures of the NO_2 production process.

Table 4.5: Control performance of the industrial process.

Sample intervals	FF payout measure η_{FF}	FB only performance η^*_{FB+FF}	FB+FF performance η_{FB+FF}	Performance improvement $\frac{\eta_{FB+FF}-\eta^*_{FB+FF}}{\eta^*_{FB+FF}} \times 100\%$
1200 - 3500	0.0176	0.210	0.215	2.40
3600 - 4000	0.317	0.0713	0.181	154
4000 - 6200	0.00576	0.169	0.194	14.6
6300 - 6700	0.913	0.0129	0.237	1.74×10^3

only 1.76 and 0.576 percent of the total variance respectively.

The high payout measure during the periods from 3600 to 4000 and 6300 to 6700 sample intervals, on the other hand, indicates that the fluctuations in ammonia temperature contributes significantly to the variance of the catalyst temperature (31.7 and 91.3 percent respectively). As seen in the bottom graph of Figure 4.6, the magnitude of this infrequent disturbance is greater than the continuous noise. So the payout measure and the percentage performance improvement are expected to be higher whenever the fluctuations occur. Removing these fluctuations by implementing feedforward control is potentially effective in reducing process variability. It is, therefore, worthwhile to incorporate a feedforward controller into the existing system if wide fluctuations occur frequently, or if these fluctuations cause fatal consequences to the process. Note that the feedback plus feedforward control performance index will still be low ($\eta_{FB+FF} \simeq 0.2$). This small index indicates that the tuning of the feedback controller is relatively poor.

4.7 Conclusions

Feedforward controllers improve control loop performance by reducing or eliminating the effect of measurable disturbances. Implementing feedforward control, however, is feasible if and only if the measurable disturbance has relatively significant effect on the

process output. A payout measure which estimates the contribution of a measurable disturbance to the process variance is introduced in this chapter. It serves as a useful tool to evaluate the potential benefit from implementing feedforward control to an existing feedback system. Performance prediction of the future feedback plus feedforward is also discussed. The proposed performance analysis is demonstrated by simulations, on a pilot scale process and an industrial process. The industrial application of the analysis confirms the conclusions made in the previous two chapters: the poor performance of the reactor control loop in the NO_2 production process is caused by the wide fluctuations in the ammonia temperature. It is also concluded that feedforward control scheme could be considered to remove these fluctuations in order to reduce the process variability.

Chapter 5

Sensitivity of Feedback Control Performance Measure to Time Delay Mismatch

5.1 Introduction

Minimum variance control serves as a useful benchmark for assessing control loop performance. One of the most important pieces of information required for this performance assessment method is the process delay. It is defined as the number of control intervals elapsed between a change in the manipulated variable and its effect on the process output. Process delay can usually be obtained from an open loop step test; however, this test is generally undesirable due to the risk of production upsets. Despite this, a rough estimate of the process delay is often accessible from experienced personnel.

The feedback control performance measure defined in Chapter 3 is a function of the process delay d. Thus, its accuracy in indicating the control loop performance depends on the precision of the estimate of d. If d is poorly estimated, the performance measure may not reflect the true feedback controller performance, and the indicated potential for improvement by retuning the controller may be incorrect. Therefore, it

would be of interest to investigate the sensitivity of the performance measure to the accuracy of d.

In this chapter, the effect of the delay mismatch on the performance index, $\eta(d)$, is discussed via a simulation example. The performance index curve or PI curve is introduced to study the sensitivity of $\eta(d)$ to the delay mismatch $\left| d - \widehat{d} \right|$. The 95% confidence level bound is also used to determine how accurate the estimated measure is.

5.2 Over- and Under-estimation of Process Delay

In Chapter 3, the feedback control loop performance index $\eta(d)$ is defined as the sum of the squared cross correlation coefficients of y_t and a_t between lags 0 to $d - 1$, or

$$\eta(d) = \rho_{ya}^2(0) + \rho_{ya}^2(1) + \cdots + \rho_{ya}^2(d - 1) \tag{5.1}$$

It is obvious that the number of terms in the calculation of $\eta(d)$ depends on the process delay d. When the estimated process delay $\widehat{d}$ is over-estimated, that is if $\widehat{d} > d$, $(\widehat{d} - d)$ more terms are added to the right hand side of Equation 5.1. The calculated performance index $\eta(\widehat{d})$ is therefore greater than the actual value $\eta(d)$. On the other hand, if the delay is under-estimated, or $\widehat{d} < d$, $(d - \widehat{d})$ fewer terms are included in the calculation. In this case, $\eta(\widehat{d})$ would be smaller than $\eta(d)$.

How much $\eta(\widehat{d})$ deviates from $\eta(d)$ depends not only on how much $\widehat{d}$ differs from d, but also on the magnitude of the cross correlation terms included in or excluded from the index calculation due to inaccurate estimation of the delay. For instance, even if the delay mismatch is large, the error terms due to mismatch could still be negligible if the magnitude of the cross correlation terms is small. In this case $\eta(\widehat{d})$ would still be fairly accurate in indicating the control performance. However, if the magnitude of these terms are large, the difference between $\eta(\widehat{d})$ and $\eta(d)$ will be significant. In other words, the sensitivity of $\eta(\widehat{d})$ to process delay mismatch is dependent on the rate of decay of the cross correlation response.
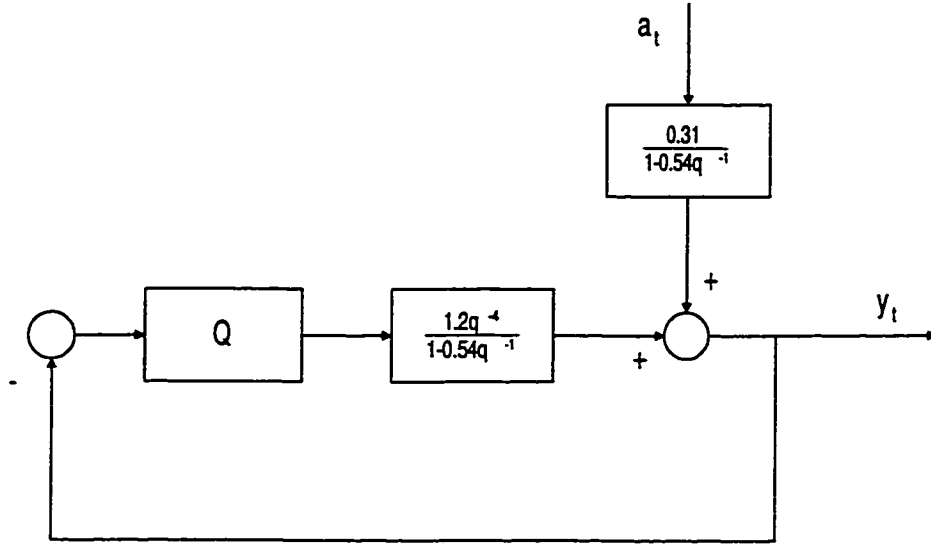
61

Figure 5.1: Block diagram of the simulated process.

For a minimum variance type controller, the performance index is not affected by the over-estimation of process delay. It is because the remaining cross correlation coefficients after the first d terms are all zero in the minimum variance case; that is, $\rho^2_{ya}(d) = \rho^2_{ya}(d+1) = \cdots = 0$. This will be illustrated in the following example.

5.3 Simulated Example

A simulated example is presented to illustrate how the index due to delay mismatch is affected by the cross correlation between y_t and a_t. Figure 5.1 shows a process under regulatory control with $d = 4$. a_t is a white noise sequence with $\sigma^2_a = 1$, and Q represents the feedback controller. Simulation runs were conducted for each of the controllers A, B, C and D, and the output responses y_t obtained. $\eta(\widehat{d})$ for each controller, estimated from the cross correlation coefficients of y_t and a_t, can be plotted against $\widehat{d}$ to form a performance index (PI) curve. The cross correlation responses and their corresponding PI curves are shown in Figures 5.2 and 5.3 respectively.

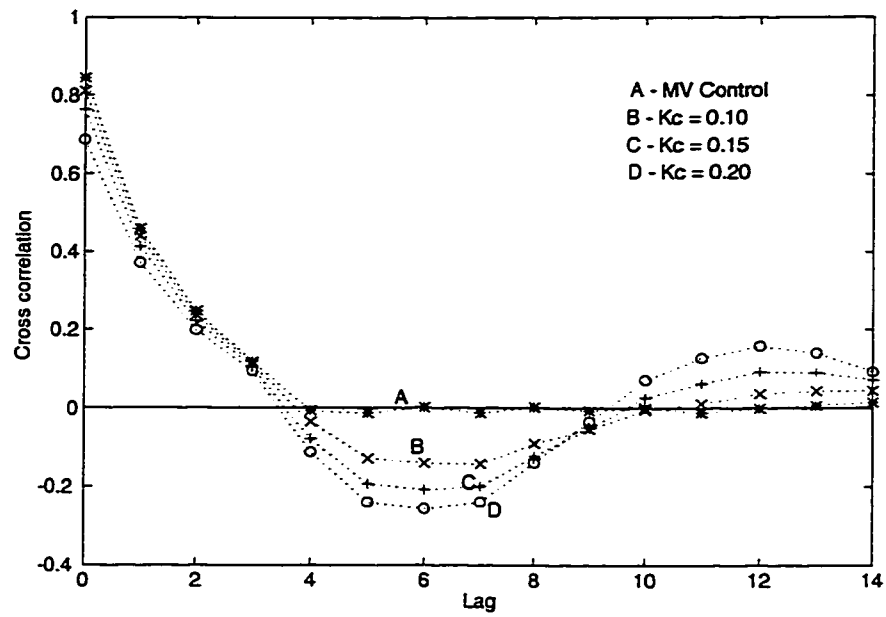Controller A in this example is a minimum variance controller. The derivation of

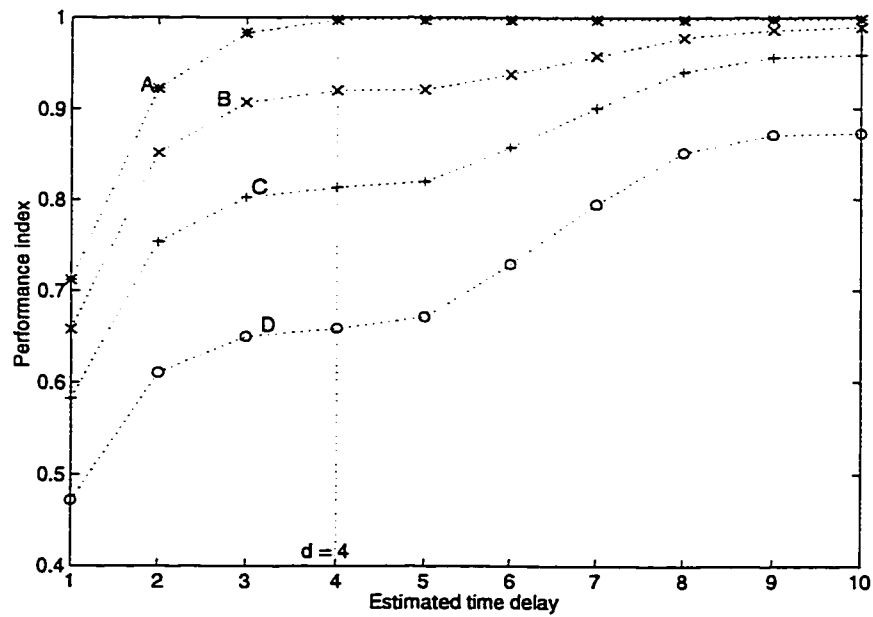Figure 5.2: Cross correlation response of the simulated process.

Figure 5.3: Performance index curve of the simulated process.

63

its control law can be found in Appendix B. Figure 5.2 shows that the cross correlation response of A decreases steadily from 0.844 at lag 0 to -6.07×10^{-3} at lag 4, and it remains close to zero thereafter. Thus, $\eta(\hat{d})$ is expected to be $\hat{d}$ invariant after lag 4. This is verified by the PI curve in Figure 5.3. The index attains a constant value after rising from 0.712 at $\hat{d} = 1$ to 0.997 at $\hat{d} = 4$. This indicates that over-estimation of process delay has minimal effect on the performance index of a minimum variance controller. In addition, one could also determine the process delay of a system with minimum variance control by plotting either the cross correlation response or the PI curve.

Controllers B, C and D are non-optimal feedback controllers of the form

$$\frac{K_c}{1 - 0.5q^{-1}}$$

with increasing controller gain K_c. The respective controller gains are shown in Table 5.1. As illustrated in Figure 5.2, a larger K_c makes the process response more oscillatory. In Figure 5.3, the increasing slope of PI curves between lags 5 and 8 for controllers B to D show that increasing K_c also makes $\eta(\hat{d})$ more sensitive to over-estimation of d. Figure 5.4 is a plot of the deviation of index, $\eta(\hat{d}) - \eta(d)$, versus delay mismatch, $(\hat{d} - d)$, with $d = 4$. The delay mismatch seems to have a more apparent effect on the index when $\left| \hat{d} - d \right| > 1$; that is, when the process delay is over- or under-estimated by more than one unit. Furthermore, as K_c increases, the deviation becomes even larger. This proves that the sensitivity of $\eta(\hat{d})$ to process delay mismatch is dependent on the rate of decay of the cross correlation response.

The PI curve shown in Figure 5.4 is also useful in the following situation. For instance, if the range of $\hat{d}$ is estimated to be [3, 5], it is unnecessary to have a more accurate estimation of the delay in order to calculate $\eta(\hat{d})$. The close performance

Table 5.1: Controller gains selected for the simulation.

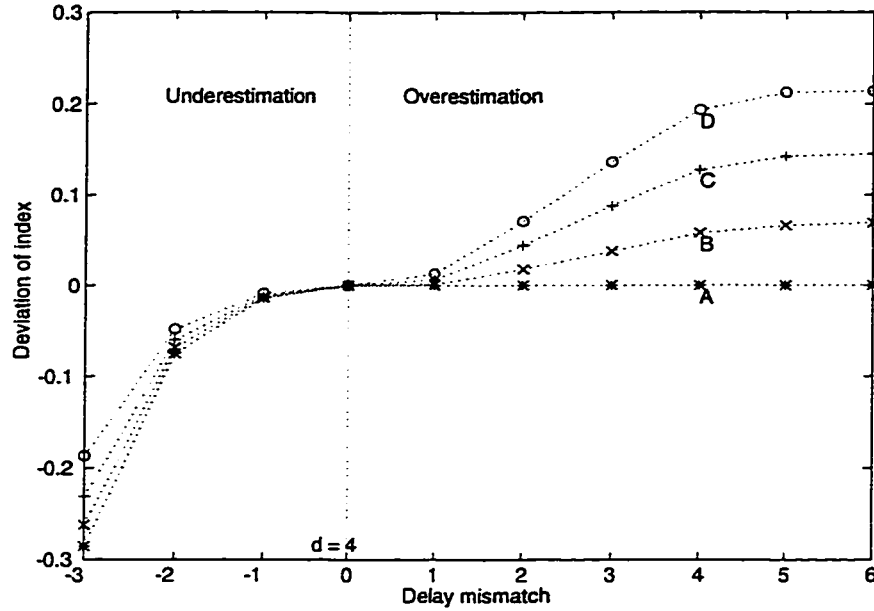| Controller	B	C	D
K_c	0.10	0.15	0.20

Figure 5.4: Effect of delay mismatch on the performance index.

measures at $\widehat{d} = 3, 4$ and 5 all provide good indications of the control performance.

5.4 Confidence Limits of the Performance Measure

While the PI curve gives an idea of how $\eta(\widehat{d})$ changes with $\left| d - \widehat{d} \right|$, it does not provide information on how accurate the measure is. In view of this, the statistical properties of the index that have been introduced in Chapter 3 are applied here to calculate the confidence intervals for the estimated index.

Figure 5.5 is the performance index curve of a closed-loop system with $d = 5$. The dash-dotted lines are the 95% bounds. The bounds get wider at bigger $\widehat{d}$ because the number of cross correlation terms taken into calculation is larger, and hence the measure becomes less accurate. $\eta(\widehat{d} = 5)$ is calculated as 0.67 ± 0.13, or $[0.54, 0.79]$. Note that the confidence bounds only indicate for a given value of d the range in which η would lie due to errors of chance, that is 95 times out of 100, within the
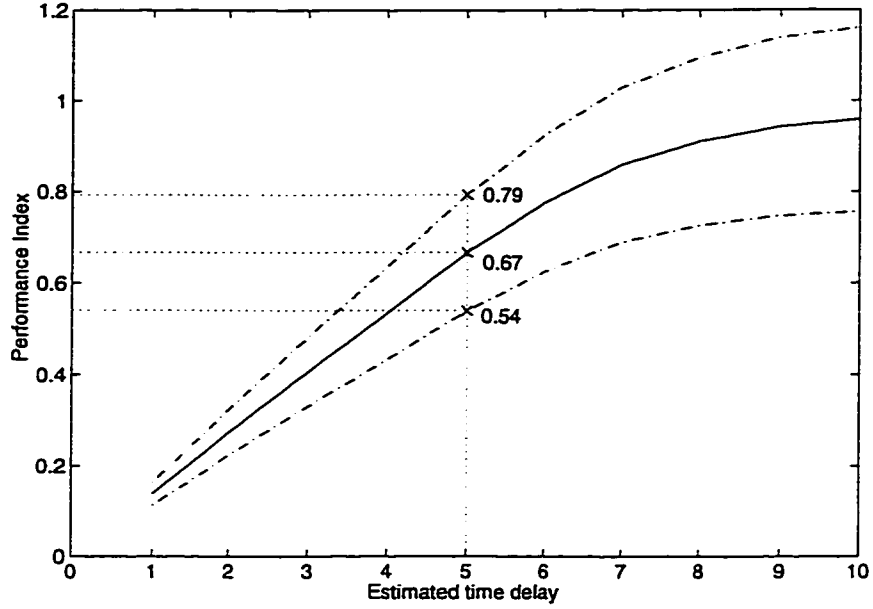
Figure 5.5: Performance index curve with 95% bounds

specified bounds. They, however, do not indicate how accurate $\widehat{d}$ is.

5.5 Conclusions

The performance measure $\eta(d)$ is a function of d. It is important to have an accurate estimate of d in order to have an index to indicate the control loop performance correctly. If the estimate of d is unreliable, the effect of the time delay mismatch should be investigated. The sensitivity of $\eta(\widehat{d})$ to $\left|\widehat{d} - d\right|$ has been discussed in this chapter. A simulation example has shown that the sensitivity is dependent on the cross correlation response of a system. The use of performance index curve and its confidence level bounds to determine the accuracy of $\eta(\widehat{d})$ has also been illustrated.

Chapter 6

Performance Assessment of Multivariate Control Systems

6.1 Introduction

Since most industrial processes are inherently multivariate in nature, performance assessment of multivariate processes has been attended and studied. Huang (1997) has developed a performance assessment algorithm for multi-input multi-output (MIMO) processes using multivariable minimum variance control as benchmark. However, the approach of Huang requires *a priori* knowledge of the MIMO time delay matrix, also called the interactor matrix. The interactor matrix, a non-trivial extension of the single-input single-output (SISO) time delay, characterizes the most fundamental performance limitation of a linear multivariable feedback system. It can be simple, diagonal or general. Determination of a simple or diagonal interactor matrix requires only information of the pure process delays. However, factorization of a general interactor matrix needs a complete knowledge or at least the first few Markov parameters of the process.

The objective of this chapter is to present a performance assessment technique which does not require any information of the interactor matrix. The strategy uses knowledge of the delays between different input-output pairs and the manipulated

inputs of the process instead. Two simulation examples are presented to demonstrate the application of the proposed technique. Results are compared to those generated from Huang's MIMO algorithm

6.2 Assessment Strategy based on Multi-loop Control Structure

Figure 6.1 shows a 2×2 multivariable process under regulatory control. The manipulated inputs and process outputs are denoted by u_j and y_i respectively. $\widetilde{T}_{ij}$ are the delay-free process transfer functions from u_j to y_i with d_{ij} as the time delays of each individual loops. N_{ij} are the transfer functions of the zero-mean white noise sequences a_j to y_i. Q_i are the feedback controllers for the two loops. It follows from Figure 6.1 that

$$\underline{y}(t) = \mathbf{T}\underline{u}(t) + \mathbf{N}\underline{a}(t) \qquad (6.1)$$

where $\underline{y} = [y_1 \ y_2]'$, $\underline{u} = [u_1 \ u_2]'$, and $\underline{a} = [a_1 \ a_2]'$.

The MIMO performance assessment method of Huang (1997) is to view the system as a whole and develop multivariable minimum variance control benchmark from Equation 6.1. The procedure uses the unitary interactor extracted from $\mathbf{T}$ to represent the limitation on the achievable performance of the multivariable feedback controller. Hence, the strategy requires *a priori* knowledge of the interactor matrix.

In order to avoid dealing directly with the interactor matrix, an alternate approach is proposed to develop for assessing performance of MIMO systems. The control performance of the system shown in Figure 6.1 is investigated one loop at a time. For the first loop, output y_1 is expressed as following:

$$y_1(t) = \frac{q^{-d_{12}}\widetilde{T}_{12}}{1 + q^{-d_{11}}\widetilde{T}_{11}Q_1}u_2(t) + \frac{N_{11}}{1 + q^{-d_{11}}\widetilde{T}_{11}Q_1}a_1(t) + \frac{N_{12}}{1 + q^{-d_{11}}\widetilde{T}_{11}Q_1}a_2(t) \qquad (6.2)$$

Assume the effect of a_2 on y_1 is very small, that is, $N_{12} \simeq 0$. Then Equation 6.2 is simplified to

$$y_1(t) = \frac{q^{-d_{12}}\widetilde{T}_{12}}{1 + q^{-d_{11}}\widetilde{T}_{11}Q_1}u_2(t) + \frac{N_{11}}{1 + q^{-d_{11}}\widetilde{T}_{11}Q_1}a_1(t) \qquad (6.3)$$
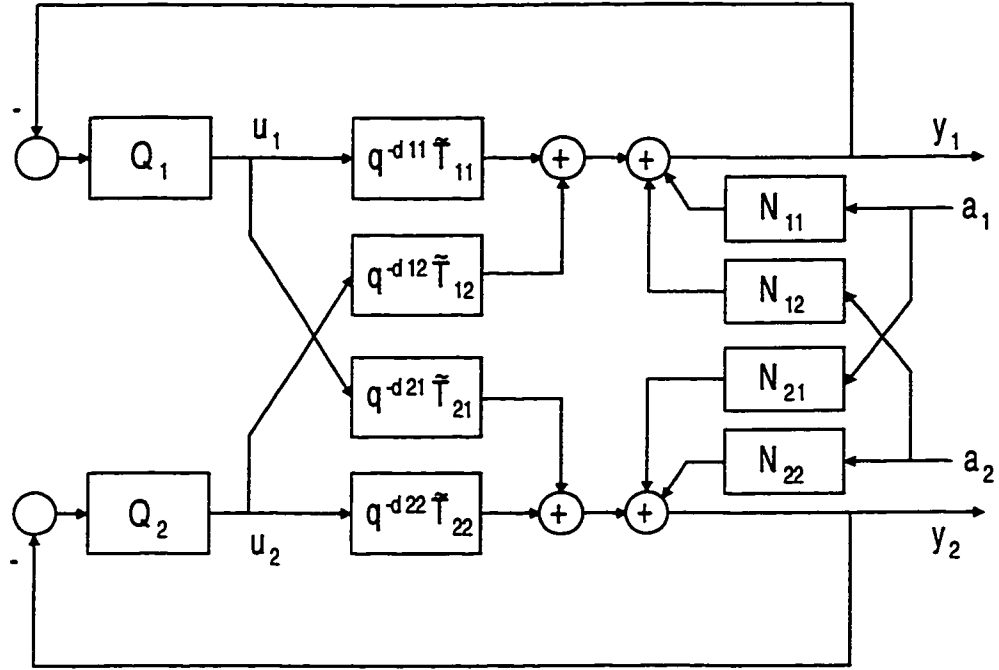
Figure 6.1: Block diagram of a 2 × 2 closed-loop system.

This information, that is the weak interaction between a_2 and y_1, may be available through *a priori* knowledge of the process. In the absence of this information, the performance of the multivariate controller cannot be estimated without the knowledge of the interactor. The first term in Equation 6.3 represents the loop interaction between u_2 and y_1.

In the special case when $\tilde{T}_{12}$ equals zero, there will be no interaction between u_2 and y_1, and Equation 6.3 will simply become

$$y_1(t) = \frac{N_1}{1 + q^{-d_{11}}\tilde{T}_{11}Q_1}a_1(t) \tag{6.4}$$

In this case, the univariate FCOR algorithm introduced in Chapter 3 can be applied to evaluate the performance index of the loop.

For cases with $\tilde{T}_{12} \neq 0$ and is significant, the univariate FCOR algorithm will not be able to provide an accurate estimation of the innovations sequence $\hat{a}_1$. Hence, the calculated performance index will be inaccurate. Since u_2 is usually known or measurable, it could be utilized to estimate $\hat{a}_1$. The procedure is similar to the

one used for calculating feedforward payout measure in Chapter 4 except that the measurable disturbance b_t is now replaced by u_2. The closed-loop transfer functions between y_1 and u_2 in Equation 6.3 can be identified using time series models. Note that d_{12} is required in this identification step. With the model available, it is then possible to estimate $\widehat{a}_1$ from the residual term. The final step would be to evaluate the performance index based on the following equation:

$$\eta(d_{11}) \triangleq \frac{\sigma^2_{mv_1}}{\sigma^2_{y_1}} = \rho^2_{y_1\widehat{a}_1}(0) + \rho^2_{y_1\widehat{a}_1}(1) + \cdots + \rho^2_{y_1\widehat{a}_1}(d_{11} - 1) \tag{6.5}$$

where $\rho^2_{y_1\widehat{a}_1}(k)$ is the cross correlation coefficient between y_1 and $\widehat{a}_1$.

This technique actually simplifies a MIMO problem into a MISO system, with u_2 and a_1 as the inputs and y_1 as the only output. The loop interaction is taken care of while estimating $\widehat{a}_1$ with this MISO method. Another advantage of this algorithm is that no information of the interactor matrix is required. All it needs is *a priori* knowledge of the delays d_{ij} between different input-output pairs of the process. This procedure can be repeated for the remaining outputs.

6.3 Simulation Examples

In order to compare the univariate FCOR algorithm and the proposed MISO method with Huang's MIMO algorithm, two examples of 2×2 processes with open loop transfer function matrix **T** and disturbance transfer function matrix **N** are studied. In each example, $\underline{a}$, a two-dimensional normally-distributed white noise sequence with $\Sigma_a = I$ and a multi-loop controller without interaction compensation

$$\mathbf{Q} = \begin{bmatrix} \frac{0.5 - 0.2q^{-1}}{1 - 0.5q^{-1}} & 0 \\ 0 & \frac{0.25 - 0.2q^{-1}}{(1 - 0.5q^{-1})(1 + 0.5q^{-1})} \end{bmatrix}$$

are used. Process gains are altered to generate different process conditions for investigation.

Although Huang's method is used, only the performance measure of each individual control loop is calculated and compared. His measure of the overall performance of all the outputs will not be calculated or discussed here.

70

Example 1: This example illustrates the effect of process interaction on the SISO and the MISO indices.

In this example, $\mathbf{T}$ and $\mathbf{N}$ are given as

$$\mathbf{T} = \begin{bmatrix} \frac{q^{-1}}{1-0.4q^{-1}} & \frac{K_{12}q^{-2}}{1-0.1q^{-1}} \\ \frac{K_{21}q^{-1}}{1-0.3q^{-1}} & \frac{q^{-2}}{1-0.8q^{-1}} \end{bmatrix}$$

$$\mathbf{N} = \begin{bmatrix} \frac{1}{1-0.4q^{-1}} & 0 \\ 0 & \frac{1}{1-0.3q^{-1}} \end{bmatrix}$$

K_{21} is arbitrarily set at 0.2, 0.4 and 0.7, and the corresponding unitary interactor matrices $\mathbf{D}$ can be determined as:

$$\mathbf{D} = \begin{bmatrix} -0.981q & -0.196q \\ -0.196q^2 & 0.981q^2 \end{bmatrix} \text{ for } K_{21} = 0.2,$$

$$\mathbf{D} = \begin{bmatrix} -0.928q & -0.371q \\ -0.371q^2 & 0.928q^2 \end{bmatrix} \text{ for } K_{21} = 0.4,$$

$$\mathbf{D} = \begin{bmatrix} -0.819q & -0.573q \\ -0.573q^2 & 0.819q^2 \end{bmatrix} \text{ for } K_{21} = 0.7$$

For each of the three cases when $K_{21} = 0.2, 0.4$ and 0.7, K_{12} is varied from 0 to 10 to increase process interaction. The calculated indices are plotted against K_{12} to determine the effect of interaction.

Figure 6.2 shows the result for $K_{21} = 0.2$. Performance assessment techniques, namely MIMO and SISO, are applied separately on y_1 and y_2. The performance indices calculated by MIMO technique are denoted by 'o', whereas those estimated with SISO technique is represented by '*'. The dash-dotted and the dotted lines distinguish the performance indices of y_1 and y_2 respectively.

From Figure 6.2, when K_{12} is zero, both multivariate and univariate performance measures are close to unity indicating good control loop performance due to the weak interaction of the control loops. Furthermore, the univariate measure is close to the multivariate measure at $K_{12} = 0$. However, as interaction, or equivalently,

K_{12} increases, the performance deteriorates. This is especially noticeable in y_1. The multivariate measure of y_1 drops rapidly because of its high sensitivity to the increase in control loop interaction caused by changes in K_{12}. Even though the multivariate and the univariate measures are still close for y_2, the two measures of y_1 deviate significantly. This is due to the fact that loop interactions of the system is ignored when applying the univariate FCOR algorithm.

The proposed MISO method is now applied to the same system and is compared to the MIMO technique. Figure 6.3 shows the performance curves generated using these two strategies. As observed from the figure, there is a good match between the indices calculated by the MISO and the MIMO algorithms for both y_1 and y_2. Even though the loop interactions become stronger when K_{12} increases, the MISO algorithm still provides accurate measure on the control performance.

Same comparisons are made for the other two cases: $K_{21} = 0.4$ and 0.7. The calculated performance indices are plotted in Figures 6.4, 6.5, 6.6 and 6.7. As before, the dash-dotted and the dotted lines represent the performance of y_1 and y_2 respectively. For the case of $K_{21} = 0.7$, the system becomes unstable as K_{12} increases beyond 7, and therefore the simulation stops at $K_{12} = 7$.

Figures 6.4 and 6.6 indicates that the deviation between the two measures becomes more obvious in y_2 as the interaction of the second loop increases. As K_{12} increases, the deviation at y_1 becomes more significant. This again proves that univariate technique is not applicable to processes with strong loop interaction. In addition, multi-loop controllers no long perform well under the influence of loop interactions, and hence performance of both loops deteriorates as K_{12} increases.

On the other hand, the MISO method provides result that agrees to the MIMO FCOR algorithm regardless of loop interaction. Figures 6.5 and 6.7 show once again that the MISO technique is reliable in estimating control performance of multi-loop processes.
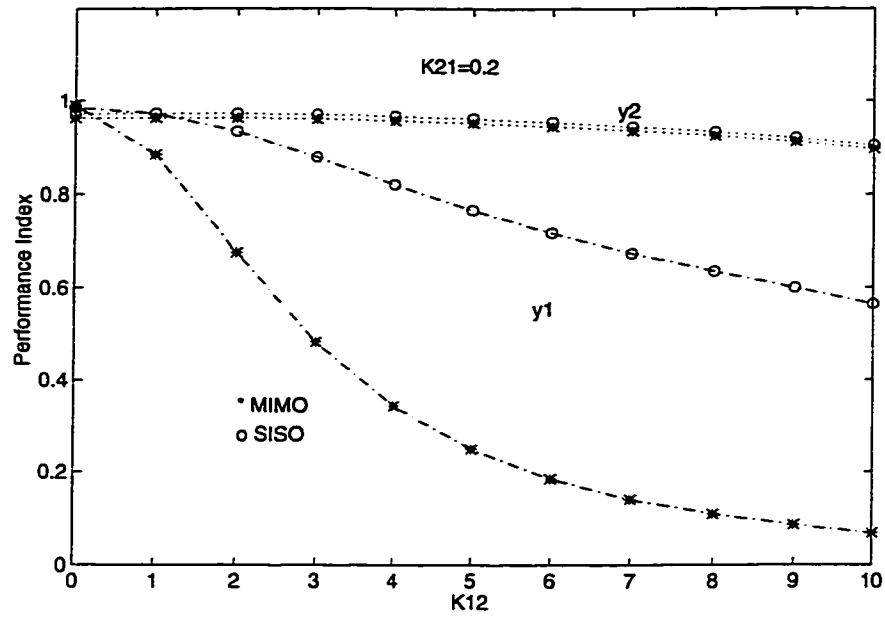
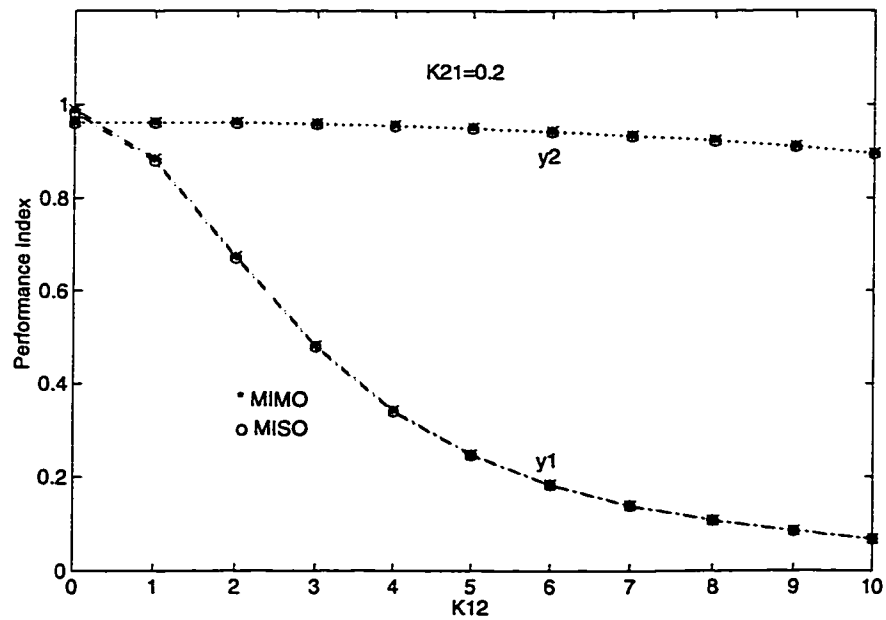Figure 6.2: Comparison of SISO and MIMO performance assessment methods for $K_{21} = 0.2$.

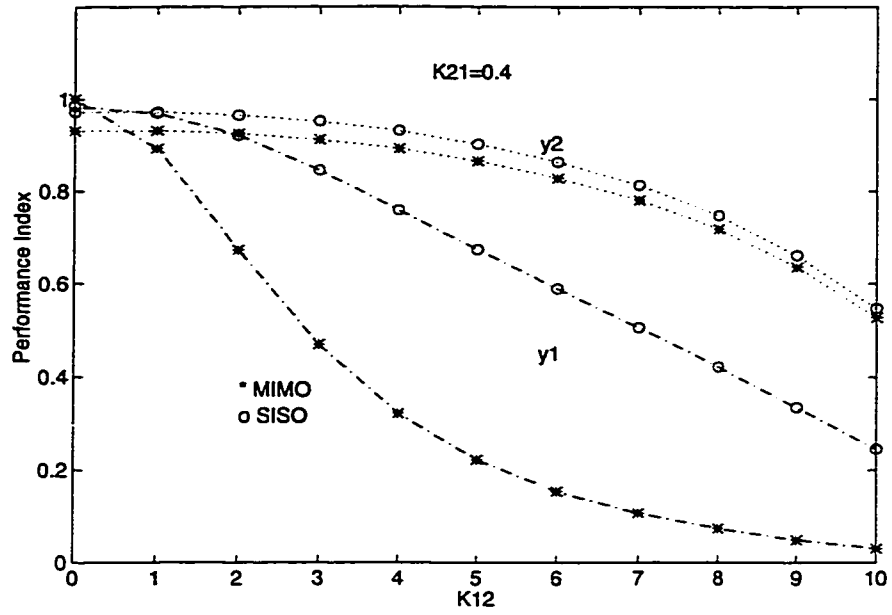Figure 6.3: Comparison of MISO and MIMO performance assessment methods for $K_{21} = 0.2$.

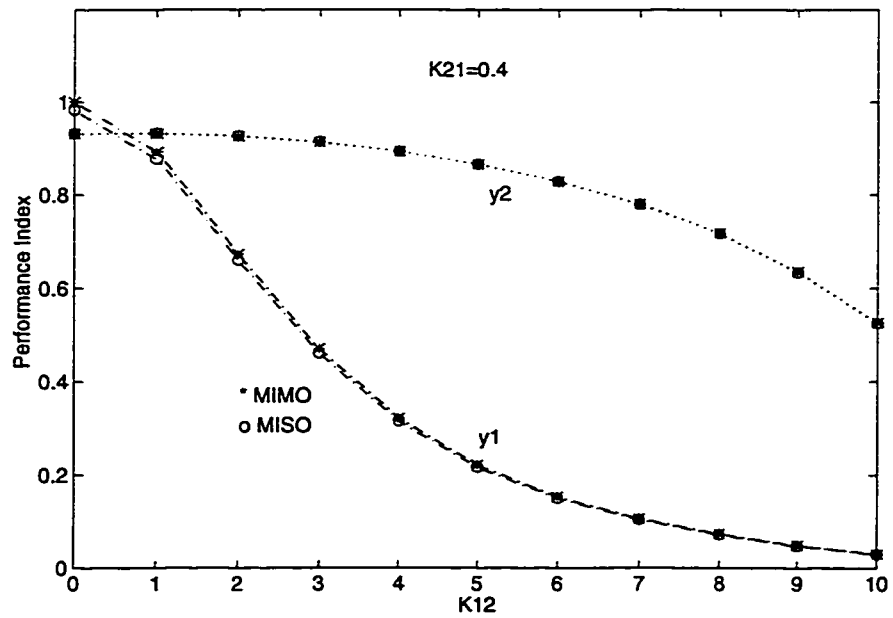Figure 6.4: Comparison of SISO and MIMO performance assessment methods for $K_{21} = 0.4$.

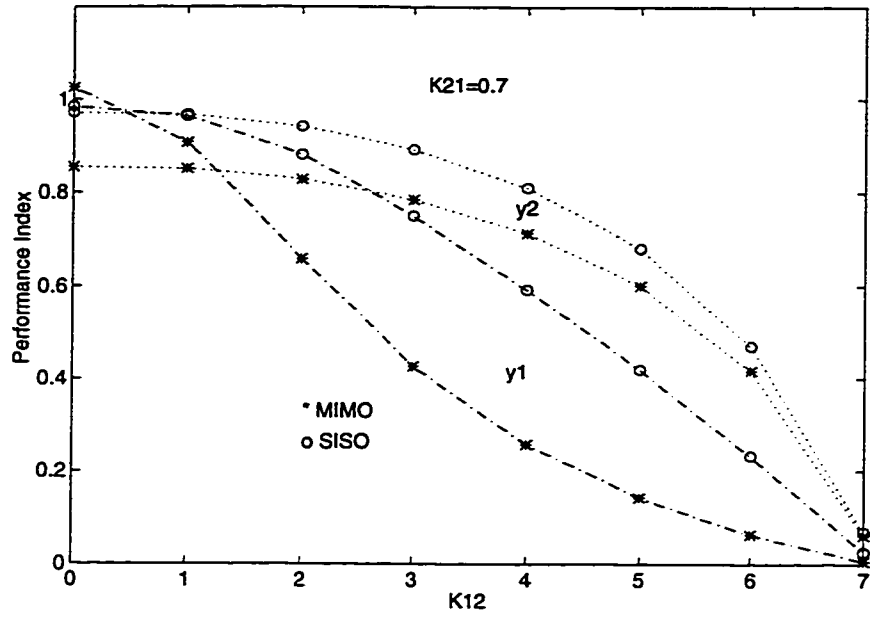Figure 6.5: Comparison of MISO and MIMO performance assessment methods for $K_{21} = 0.4$.

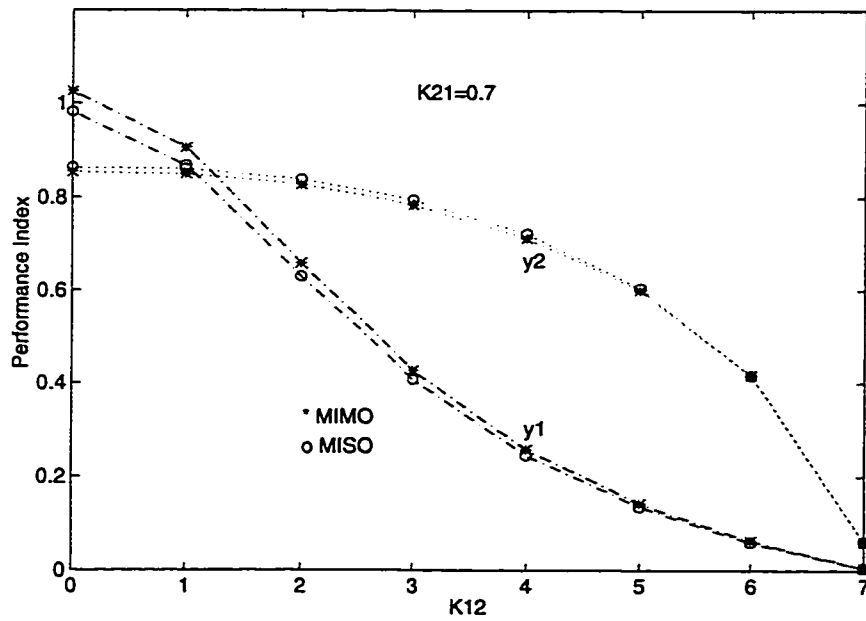Figure 6.6: Comparison of SISO and MIMO performance assessment methods for $K_{21} = 0.7$.

Figure 6.7: Comparison of MISO and MIMO performance assessment methods for $K_{21} = 0.7$.

Table 6.1: Values of n_{12} and n_{21} for Example 2.

Case	n_{12}	n_{21}
a	0.2	0.0
b	0.5	0.0
c	0.8	0.0
d	0.0	0.2
e	0.0	0.5
f	0.0	0.8
g	0.8	0.8

Example 2: This example illustrates the effect of interaction between disturbances on the MISO index.

In this example, T and N are given as

$$
T = \begin{bmatrix} \frac{q^{-1}}{1-0.4q^{-1}} & \frac{K_{12}q^{-4}}{1-0.1q^{-1}} \\ \frac{0.2q^{-1}}{1-0.3q^{-1}} & \frac{q^{-5}}{1-0.8q^{-1}} \end{bmatrix}
$$

$$
N = \begin{bmatrix} \frac{1}{1-0.4q^{-1}} & \frac{n_{12}}{1-0.5q^{-1}} \\ \frac{n_{21}}{1-0.5q^{-1}} & \frac{1}{1-0.3q^{-1}} \end{bmatrix}
$$

where n_{12} and n_{21} are selected differently as shown in Table 6.1. K_{12} varies from 1 to 10 in each case as in the previous example. The unitary interactor matrix D in all cases is approximately equal to:

$$
D = \begin{bmatrix} 0.019q^3 - 0.196q^4 & 0.004q^3 + 0.980q^4 \\ 0.980q + 0.004q^2 & 0.196q - 0.019q^2 \end{bmatrix}
$$

The indices calculated from MIMO and MISO methods are plotted against K_{12} to demonstrate the effect of increasing interaction within N. Figures 6.8 to 6.14 show the results of each case respectively.

Comparison of these figures reveals the significant effect of the interaction between disturbances on the accuracy of MISO method. When the disturbance interaction n_{12}
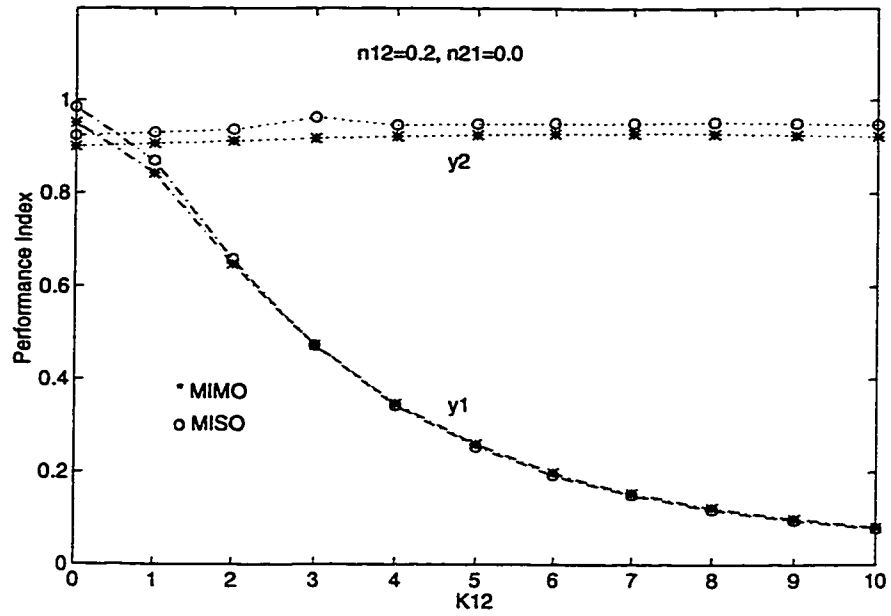
76

Figure 6.8: Comparison of MISO and MIMO performance assessment methods for $n_{12} = 0.2$ and $n_{21} = 0.0$.

Figure 6.9: Comparison of MISO and MIMO performance assessment methods for $n_{12} = 0.5$ and $n_{21} = 0.0$.

Figure 6.10: Comparison of MISO and MIMO performance assessment methods for $n_{12} = 0.8$ and $n_{21} = 0.0$.

Figure 6.11: Comparison of MISO and MIMO performance assessment methods for $n_{12} = 0.0$ and $n_{21} = 0.2$.

Figure 6.12: Comparison of MISO and MIMO performance assessment methods for $n_{12} = 0.0$ and $n_{21} = 0.5$.
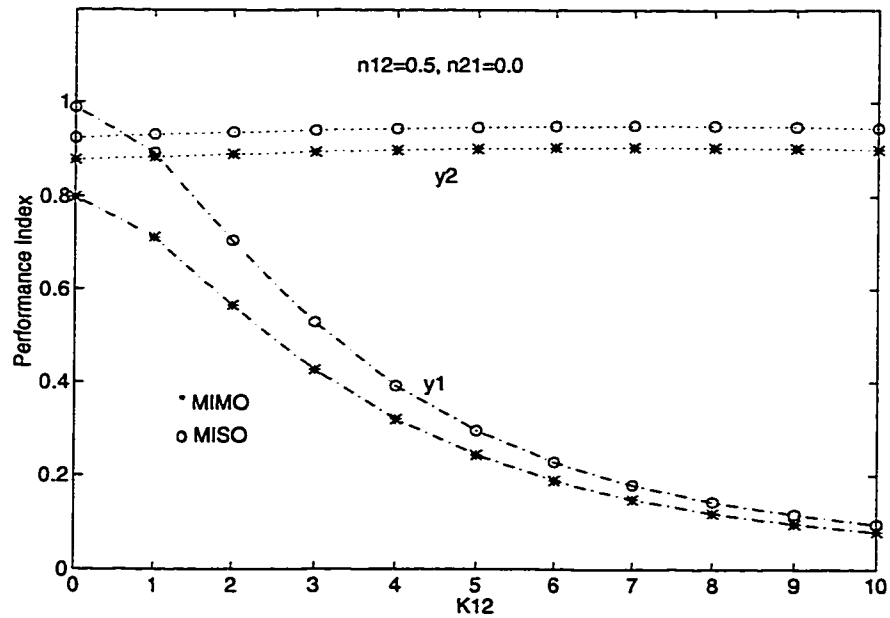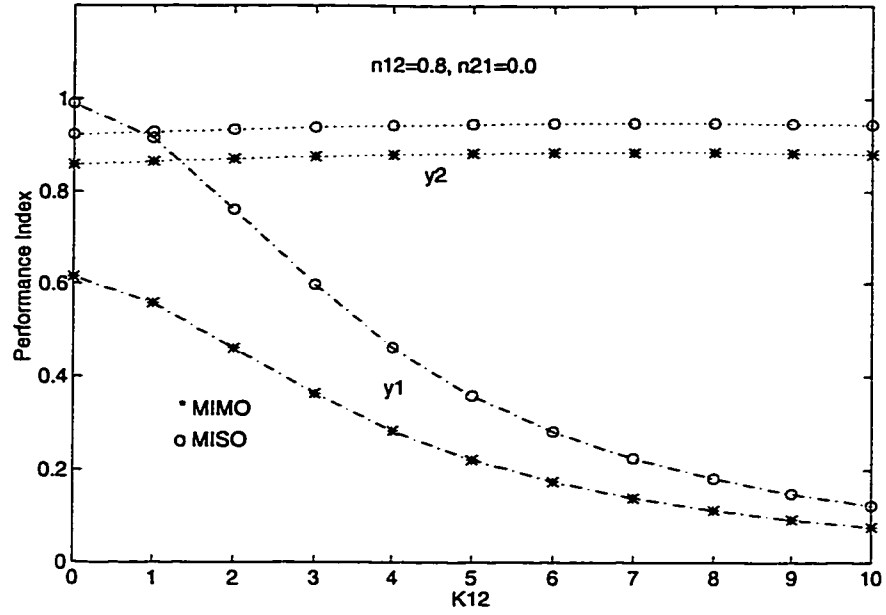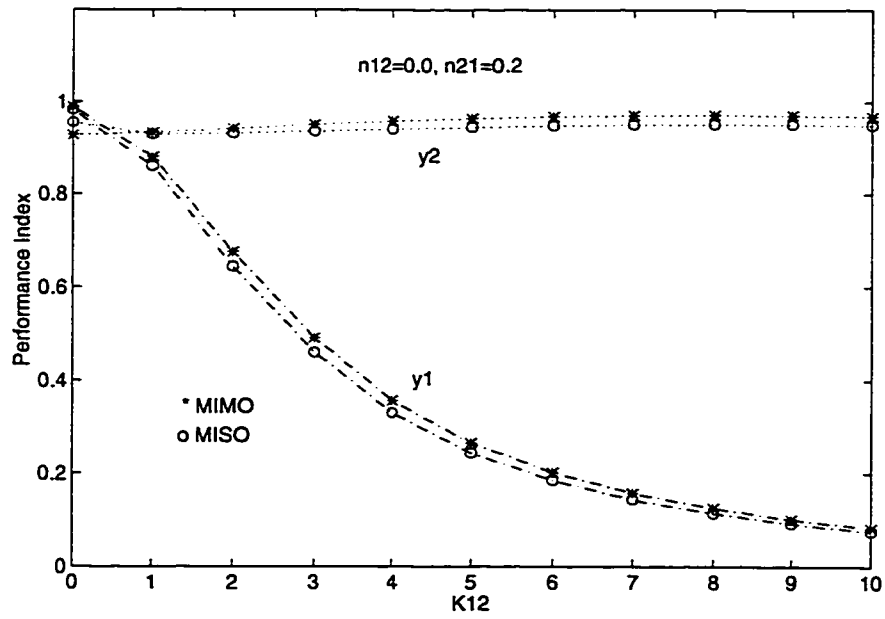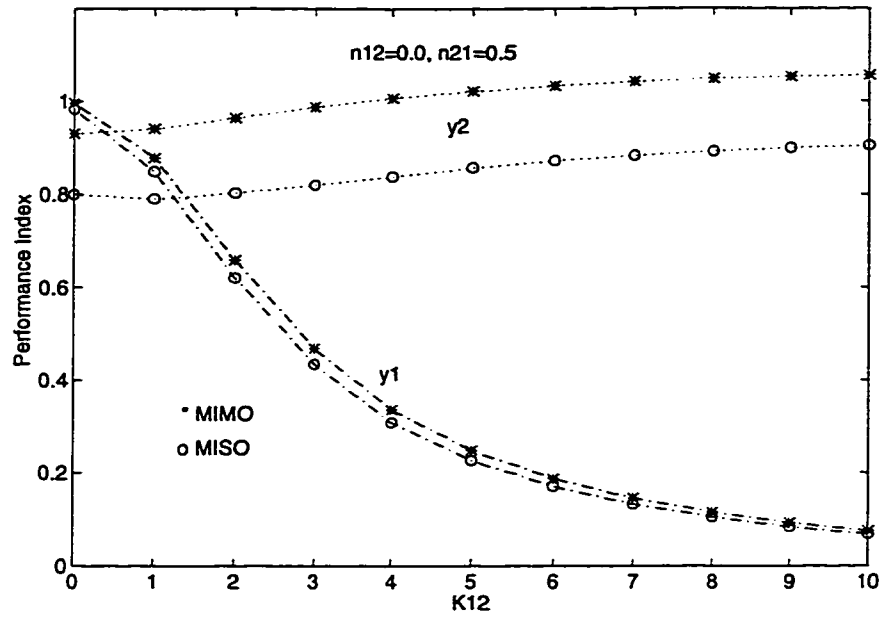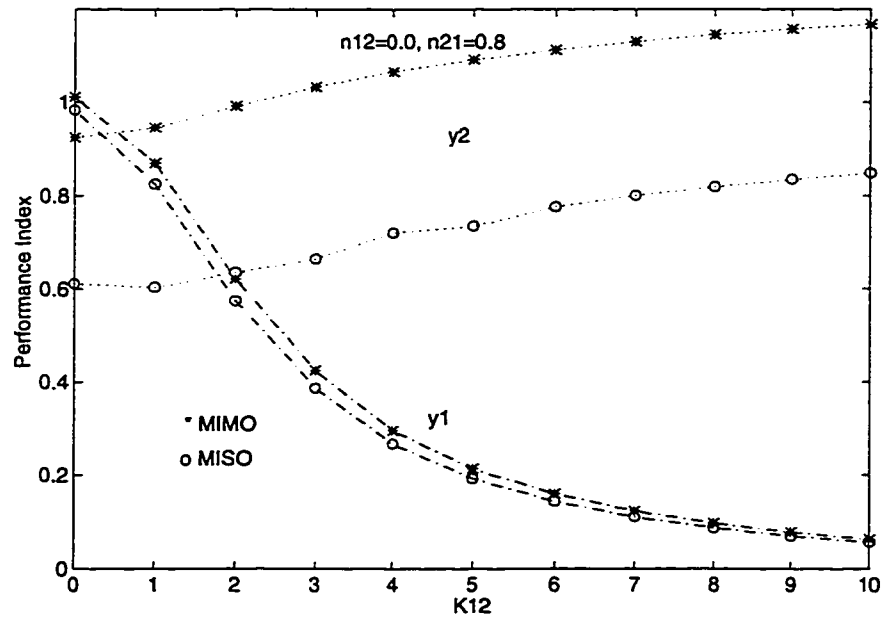

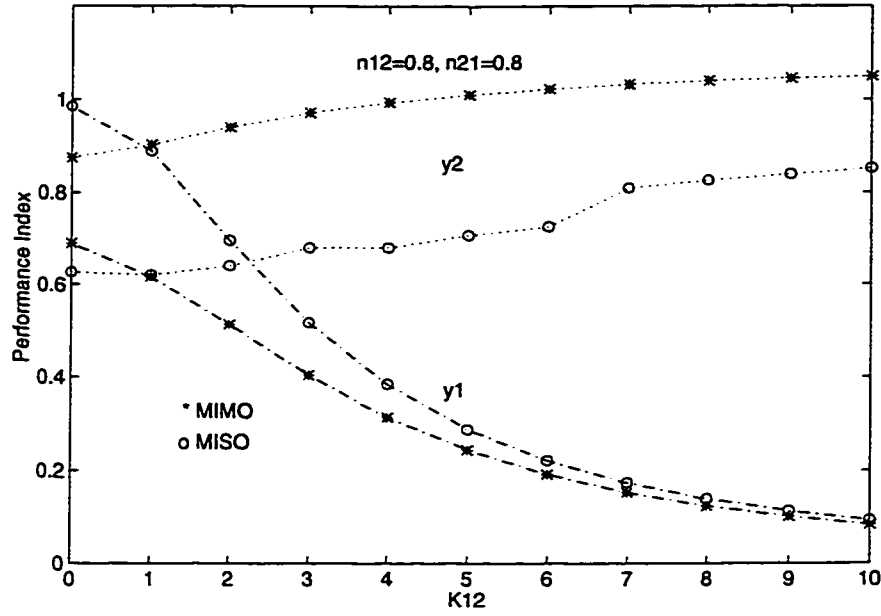Figure 6.13: Comparison of MISO and MIMO performance assessment methods for $n_{12} = 0.0$ and $n_{21} = 0.8$.

Figure 6.14: Comparison of MISO and MIMO performance assessment methods for $n_{12} = 0.8$ and $n_{21} = 0.8$.

is small in (a), the MISO indices of both y_1 and y_2 still match the MIMO indices. As n_{12} increases while keeping n_{21} zero in (b) and (c), the MISO indices of y_1 start to deviate from the MIMO indices. Performance indices of y_2 are also affected due to the two-way loop interaction of the process. The deviation originates from the assumption made when developing the MISO strategy that interaction between disturbances is negligible. Since the effect of a_2 on y_1 is no long negligible, using the MISO method to calculate the performance index will not be accurate. It is also interesting to see that as K_{12} increases, the gap between the two types of indices tightens. This is due to the fact that a_2 becomes relatively less significant on y_1 as K_{12} increases.

Similarly, as n_{21} increases while keeping n_{12} zero in (d), (e) and (f), the MISO indices of y_2 begin to deviate from the MIMO indices. As the effect of a_1 on y_2 becomes significant, the MISO method cannot be used to provide the performance measure of the process.

Figure 6.14 shows that when the interaction between the disturbances is strong

both ways, the MISO indices of both y_1 and y_2 do not agree to the MIMO indices. Therefore, whenever the interaction due to disturbances is strong, Huang's MIMO algorithm should be used to obtain control performance information.

6.4 Conclusions

Huang's MIMO FCOR algorithm provides a means of assessing control performance for MIMO systems using multivariable minimum variance control as benchmark. However, the knowledge of the unitary interactor matrix poses difficulties for this technique to be applied. In this chapter another technique which does not require any information of the interactor matrix is presented. Instead of using *a priori* knowledge of the interactor matrix, this technique uses only knowledge of the delays between different input-output pairs and the manipulated inputs of the process. It is shown via simulation that the proposed performance assessment technique generates results that agree to those of the MIMO performance assessment technique when interaction due to the disturbances is insignificant.

Chapter 7

Conclusions and Recommendations

7.1 Conclusions

Process variations exist in almost all variables in an industrial environment. It is therefore important to have effective tools for monitoring and extracting information from these variations in order to improve quality control. In this thesis, methods for process monitoring and control performance assessment are presented and discussed.

The methods outlined in Chapter 2 are useful for process monitoring. Basic statistical concept, quality control charts and sophisticated time series analysis techniques in both time and frequency domains can be used together to detect and identify major sources of variations on-line or off-line.

Other than external sources of disturbances, process variations can be caused by poor tuning in controllers. In order to distinguish between these two causes, the univariate performance assessment technique presented in Chapter 3 can be utilized. This technique uses minimum variance control as benchmark to define a normalized performance measure for feedback control. The interpretation of this performance measure is useful for establishing whether process variations can be reduced by controller retuning, or should other control schemes or reconfiguration of the process be considered. If feedforward control is being considered for removing or reducing the effect of a measurable disturbance, the payout measure introduced in Chapter 4 would

be helpful in determining the feasibility of implementing feedforward control to an existing feedback system. The analysis of variance allows the variance contributions of the measurable and the unmeasurable disturbances which enter the process to be evaluated. At the same time, the potential benefits from implementing a feedback plus feedforward control scheme can also be estimated by calculating the performance index of the future feedback plus feedforward control system.

One of the most important pieces of information required for the univariate performance assessment method of Chapter 3 is the process delay. However, the process delay, which could have a significant effect on the accuracy of the performance measure, is usually obtained through a rough estimate from experienced personnel. In this case, plotting the performance index curve as discussed in Chapter 5 would be useful to obtain information on how dependent the performance measure is on the process delay mismatch. The 95% confidence level bound given in Chapter 3 can also be used to determine the accuracy of the measure.

In industries where most processes are inherently multivariate in nature, the MISO performance assessment strategy described in Chapter 6 would be of practical use. With estimates of the delays between different input-output pairs and the manipulated input of the process available, and by assuming the interaction between disturbances to be negligible the performance indices of the control loops can be easily calculated. It has been shown that this MISO technique generates results that agree to those of the MIMO performance assessment technique without requiring the knowledge of the unitary interactor matrix if the interaction of the disturbances is insignificant.

7.2   Recommendations

1. The application of the MISO performance assessment method introduced in this thesis produces results that are close to the MIMO performance assessment without the knowledge of the interactor matrix. However, it is restricted

to processes with minimal interaction between disturbances. To extend the strategy to processes with strong interaction between disturbances, it would be worth exploring if information about disturbances from other control loops could be obtained from closed loop data of those loops.

2. Since the accuracy of performance measure relies on process delay estimate, it would be of interest to develop a method to estimate process delays from routine closed-loop data.

3. Although the most desirable control objective is usually to minimize process output variance in most practical control problems, it is limited by the presence of constraints on manipulated variables due to physical limitations of plant equipment such as pumps and control valves. Using minimum variance control as a benchmark may not be fair enough in assessing control performance of systems with constraints on control input. Extension of performance assessment techniques with control constraints as part of the control objectives is an area worthy of further investigation.

4. Cascade control can provide improvement over conventional feedback control when both master and slave controllers are well tuned. A method to assess controller performance of both controllers in a cascaded control structure would be appealing, especially in industry where a lot of cascade control loops exist.

References

Banerjee, P., *Robustness Issues in Long-Range Predictive Control*, Ch. 2, Ph.D. Thesis, Department of Chemical Engineering, University of Alberta, Edmonton, Canada (1996).

Barnard, G. A., "Control Charts and Stochastic Processes", *J. R. Statist. Soc.* B 21, 239-271 (1959).

Bauer, P. and P. Hackl, "The Use of MOSUMS for Quality Control", *Technometrics*, 20, 4, 431-436 (November 1978).

Box, G. E. P., W. G. Hunter and J. S. Hunter, *Statistics for Experimenters*, Ch. 17, John Wiley & Sons (1978).

Crowder, S. V. and M. D. Hamilton, "An EWMA for Monitoring a Process Standard Deviation", *Journal of Quality Technology*, 24, 1, 12-21 (January 1992).

Desborough, L. D., *Performance Assessment Measures for Univariate Control*, M.Sc. Thesis, Queen's University, Kinston, Ontario (1992).

Desborough, L. and T. Harris, "Performance Assessment Measures for Univariate Feedback Control", *The Canadian Journal of Chemical Engineering*, 70, 1186-1197 (1992).

Desborough, L. and T. Harris, "Performance Assessment Measures for Univariate Feedforward/Feedback Control", *The Canadian Journal of Chemical Engineering*, 71, 605-616 (1993).

Eriksson, P-G and A. J. Isaksson, "Some Aspects of Control Loop Performance Monitoring", *Proc. 3rd IEEE Conf. Control Applications*, 1029-1034 (1994).

Ettaleb, L., G. A. Dumont and M. S. Davies, *Performance Assessment of Single and Multivariable Feedback Controllers: a Unified Approach*, Pulp and Paper Centre, University of British Columbia, Vancouver, Canada (1997).

Ewan, W. D., "When and How to Use Cu-Sum Charts", *Technometrics* 5, 1, 1-22 (1963).

Grant, E. L. and R. S. Leavenworth, *Statistical Quality Control*, 5th edition, McGraw-Hill (1980).

Harris, T. J., "Assessment of Control Loop Performance", *The Canadian Journal of Chemical Engineering*, 67, 856-861 (October 1989).

Harris, T. J., F. Boudreau and J. F. MacGregor, *Performance Assessment of Multivariable Feedback Controllers*, Automatica, 32, 11, 1505-1518 (1996).

Harris, T. J., C. T. Seppala, P. J. Jofriet and B. W. Surgenor, *Plant-Wide Feedback Control Performance Assessment Using an Expert-System Framework*, Control Eng. Practice, 4, 9, 1297-1303 (1996).

Huang, B., *Control Loop Performance Assessment of SISO Processes*, Internal Report, Department of Chemical Engineering, University of Alberta, Edmonton, Alberta (1995).

Huang, B., *Multivariate Statistical Methods for Control Loop Performance Assessment*, Ph.D. Thesis, Department of Chemical Engineering, University of Alberta, Edmonton, Alberta (1997).

Huang, B., S. L. Shah and E. K. Kwok, "On-Line Control Performance Monitoring of MIMO Processes", *Proceedings of the 1995 American Control Conference*, Seattle, Washington, 2, 1250-1254 (June 1995).

Huang, B., S. L. Shah and E. K. Kwok, "Good, Bad or Optimal: Performance Assessment of Multivariable Processes", *Automatica*, 33, 6, 1175-1184 (June 1997).

Huang, B. and S. L. Shah, "Practical Issues in Multivariable Feedback Control Performance Assessment", *Proceedings of IFAC ADCHEM*, Banff, Alberta, 429-434 (June 1997).

MacGregor, J. F. and T. J. Harris, "The Exponentially Weighted Moving Variance", *Journal of Quality Technology* 25, 2, 106-118 (1993).

Nobleza, G. C., A. A. Roche and A. P. Croteau, "Time Series Analysis Techniques: A Practical Tool for Mill-wide Quality Improvements", *Pulp & Paper Canada* 91, 7, T280-285 (1990).

Pryor, C., "Autocovariance and Power Spectrum Analysis - Derive New Information from Process Data", *Control Engineering* 2, 103-106 (October 1982).

Seborg D. E., T. F. Edgar and D. A. Mellichamp, *Process Dynamics and Control*, John Wiley & Sons (1989).

Söderström, T. and P. Stoica, *System Identification*, Prentice Hall, UK (1989).

Stanfelj, N. A., T. E. Marlin and J. F. MacGregor, "Monitoring and Diagnosing Process Control Performance: The Single-Loop Case", *Ind. Eng. Chem. Res.*, 32, 301-314 (1993).

Vishnubhotla, A., S. L. Shah and B. Huang, "Feedback and Feedforward Performance Analysis of the Shell Industrial Closed Loop Data Set", *Proceedings of IFAC ADCHEM*, Banff, Alberta, 295-300 (June 1997).

Wei, W. W. S., *Time Series Analysis - Univariate and Multivariate Methods*, Addison-Wesley (1990).

Wetherill, G. B., *Sampling Inspection and Quality Control*, Methuen (1969).

Wolter, K. M., *Introduction to Variance Estimation*, Springer-Verlag, New York (1985).

Appendix A

Matlab code for calculating SISO feedback performance measure and its confidence bounds

```
%SISO FCOR Algorithm (with calculation of 95% bound)

%[eta,deta,etal,etau,ir] = sfcorbd(d,ndata,nfiltr,y)

% d - order of time-delay

% ndata - number of data (i.e. output) points

% nfiltr - order of armax filter

% y - output data sequence.

% eta - performance index (PI)

% etau - upper limit of PI

% etal - lower limit of PI

% deta - confidence limit

% ir - vector of impulse response coefficients
```

```
function [eta,deta,etal,etau,ir] = sfcorbd(d,ndata,nfiltr,y)

y = dtrend(y);

nn = [nfiltr,nfiltr];

th = armax(y,nn);

aa = resid(y,th);

%******************** eta *********************

eta=0;

for i=1:d

tem = corrcoef(y(i:ndata),aa(1:(ndata-i+1)));

rho(i) = tem(1,2);

eta = eta + rho(i)^2;

temp = corrcoef(y(i:ndata),y(1:(ndata-i+1)));

rhoy(i) = temp(1,2);

end

%***************** etau etal ******************

X = rho';

Rya = zeros(d);

Ry = zeros(d);

M = zeros(d);

for i = 1:d

Rya(i,1:d) = rho(i)*rho(1:d);

Ry(i,i:d) = rhoy(1:d-(i-1));

for j = 1:d

Ry(j,i) = Ry(i,j);
```

```
for t = i:j

temp1 = rho(t)*rho(i+j-t);

M(j,i) = M(j,i) + temp1;

end

end

end

for i = 1:d

for j = 1:d

M(i,j) = M(j,i);

end

end

CM = (Ry - 2*Rya + M)/ndata;

mse = 4*X'*CM*X;

deta = 2*(mse)^.5;

etau = eta + deta;

etal = eta - deta;

%***************** IR coeff ********************

for i = 1:30

temp2 = corrcoef(y(i:ndata),aa(1:(ndata-i+1)));

r(i) = temp2(1,2);

end

ir = r*(cov(y)/cov(aa))^0.5;
```

Appendix B

Derivation of minimum variance controller

A minimum variance controller is designed based on assuming the output variance after lag d is zero. In order to demonstrate the derivation of the minimum variance control equation, consider the regulatory control in Figure 3.1 again. The closed-loop response of this process is

$$y_t = \frac{N_a}{1 + q^{-d}Q\widetilde{T}} a_t \tag{B.1}$$

Let

$$N_a(q^{-1}) = F(q^{-1}) + q^{-d}R(q^{-1}) \tag{B.2}$$

where $F(q^{-1})$ is the feedback control invariant term. Then

$$y_t = \left[F(q^{-1}) + q^{-d}L(q^{-1}) \right] a_t \tag{B.3}$$

where

$$L(q^{-1}) = \frac{R - FQ\widetilde{T}}{1 + q^{-d}Q\widetilde{T}} \tag{B.4}$$

Minimum variance control is obtained when $L = 0$, or equivalently

$$R - FQ\widetilde{T} = 0 \tag{B.5}$$

Rearranging Equation B.5 gives

$$Q = \frac{R}{F\widetilde{T}}$$ (B.6)

which is the minimum variance control law.

Example

In section 5.2, an example with

$$\widetilde{T} = \frac{1.2}{1 - 0.54q^{-1}}$$
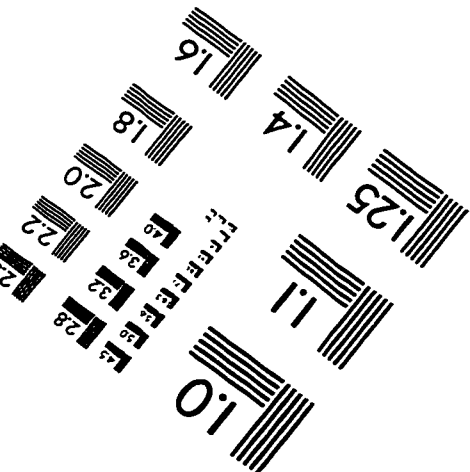
and

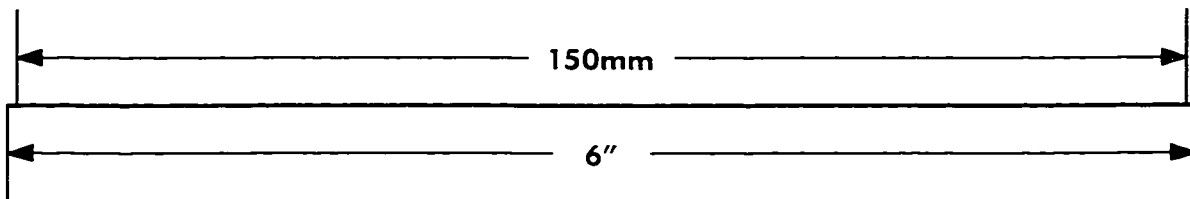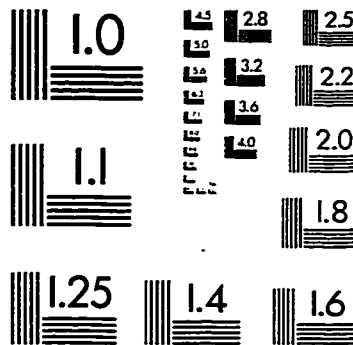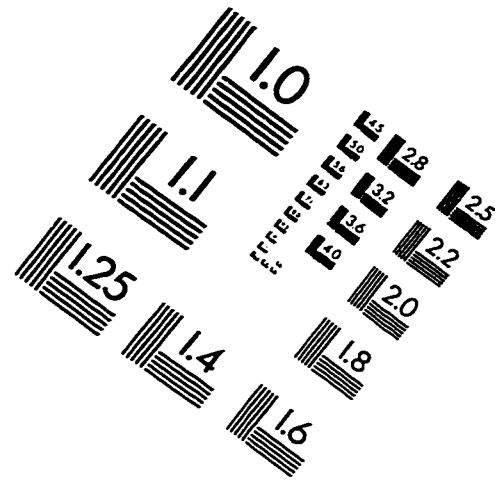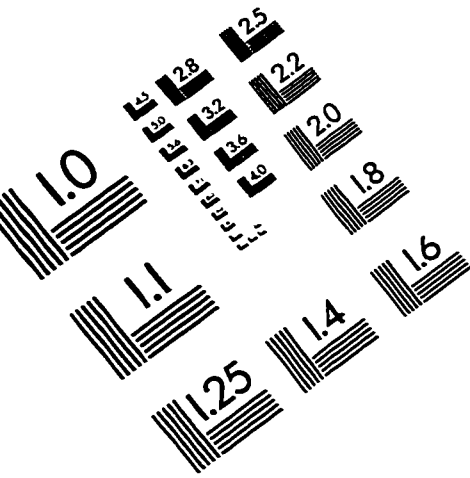$$N_a = \frac{0.31}{1 - 0.54q^{-1}}$$

was presented. N_a could be expanded into the same format as Equation B.2 as

$$N_a = \underbrace{0.31 + 0.17q^{-1} + 0.090q^{-2} + 0.049q^{-3}}_{F} + q^{-4} \underbrace{\left(\frac{0.026}{1 - 0.54q^{-1}}\right)}_{R}$$

Substituting the corresponding transfer functions into Equation B.6 yields the minimum variance controller

$$Q = \frac{0.026}{1.2(0.31 + 0.17q^{-1} + 0.090q^{-2} + 0.049q^{-3})}$$

IMAGE EVALUATION
TEST TARGET (QA-3)

150mm

6"

APPLIED IMAGE . Inc
1653 East Main Street
Rochester, NY 14609 USA
Phone: 716/482-0300
Fax: 716/288-5989